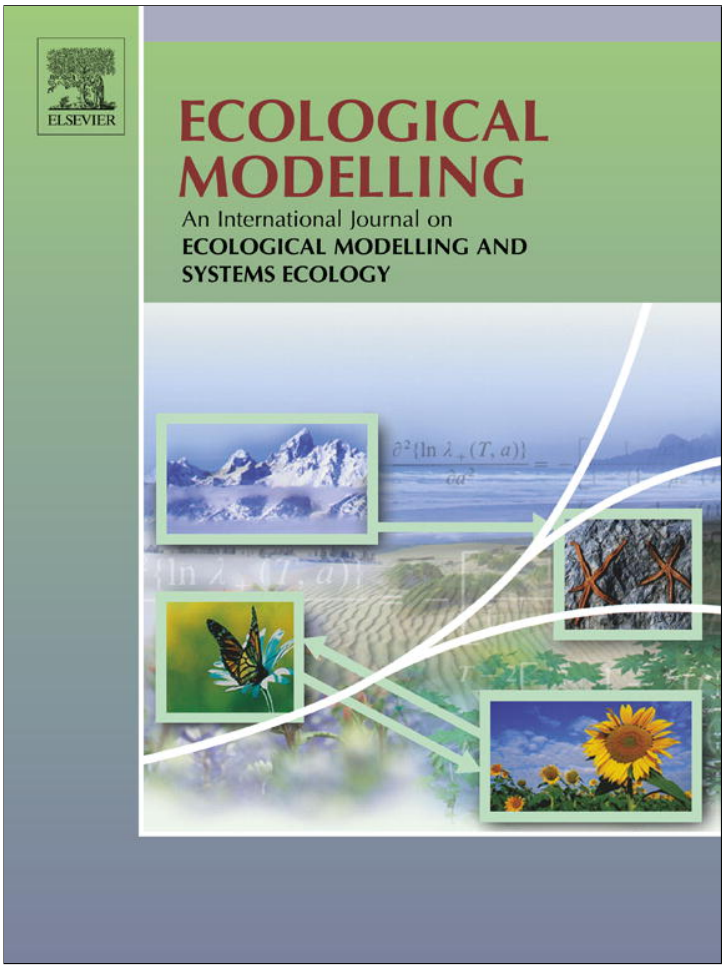

(This is a sample cover image for this issue. The actual cover is not yet available at this time.)

Ecological Modelling 240 (2012) 139–155

Contents lists available at SciVerse ScienceDirect

Ecological Modelling

journal homepage: www.elsevier.com/locate/ecolmodel

Examination of the effects of nutrient regeneration mechanisms on plankton dynamics using aquatic biogeochemical modeling

Maryam Ramin, Gurbir Perhar, Yuko Shimoda, George B. Arhonditsis*

Ecological Modeling Laboratory, Department of Physical & Environmental Sciences, University of Toronto, Toronto, Ontario M1C 1A4, Canada

ARTICLE INFO

Article history:
Received 21 February 2012
Received in revised form 12 April 2012
Accepted 17 April 2012

Keywords:
Planktonic food webs
Microbic loop
Nutrient recycling
Stoichiometry
Climate change
Aquatic biogeochemical models

ABSTRACT

The prolonged stratification of lakes due to climate warming is expected to increase the dependence of planktonic food webs on internal nutrient regeneration mechanisms (i.e., microbial mineralization, zooplankton excretion). Our current conceptualization of aquatic communities, however, suggests that while the strength of the recycling feedback loop is indeed related to climate forcing, other biotic factors (e.g., zooplankton community composition) along with the system productivity may also be equally important. What do the contemporary operational models predict about the role of recycling rates in different trophic environments? How tight is the relationship between mineralization rates and lake warming? How realistically do modelers describe the mechanisms by which nutrients in non-living organic matter are recycled into inorganic forms? Our study addresses these questions using a complex biogeochemical model that simulates multiple elemental cycles (C, N, P, Si, O), multiple functional phytoplankton (diatoms, green algae and cyanobacteria) and zooplankton (copepods and cladocerans) groups. We relaxed the assumption of strict zooplankton homeostasis by allowing nutrient use efficiency to vary with food quality. Our analysis shows that the nutrient regeneration rates can play a major role in planktonic food webs, but their relative importance is somewhat inconsistent with the existing paradigm. We provide evidence that the recycled material and the associated energy fluxes can be significant drivers in low as well as in high-productivity ecosystems depending on the period of the year examined. Warmer climatic conditions and longer stratification periods will increase the dependence of lakes on nutrient regeneration rates. The lake productivity response, however, is non-linear and non-monotonic and is modulated by the type of nutrient limitation (nitrogen or phosphorus) experienced. Our study concludes by pinpointing some problems of the existing mathematical representation of the recycling rates, and emphasizes the need to improve our understanding of the interplay among microbial metabolism, trophic state, and lake thermal structure.

1. Introduction

Nutrient cycling typically refers to the transformation of nutrients from one form to another as well as to the interplay of nutrients among organisms, habitats, or even ecosystems (Vanni, 2002). The importance of nutrient recycling in ecosystem functioning has been amply discussed in the literature over the last four decades (Odum, 1969; DeAngelis, 1992; Costanza et al., 1997; Chapin et al., 2000; Vanni, 2002). In lakes, nutrient recycling offers a plausible explanation of the paradoxical occurrence of mid- and late-summer phytoplankton blooms, when intense stratification and nutrient limitation would seem to preclude substantial algal growth (De Pinto et al., 1986; Kamarainen et al., 2009). Allochthonous loading and entrainment of nutrient-rich metalimnetic water masses are significant pathways of the epilimnetic nutrient budget on an annual basis, but mineralization of organic compounds by heterotrophic zooplankton and microbes constitutes a major source of the nutrients required to fuel phytoplankton production during the period of summer stratification and low ambient nutrient availability (Vanni, 2002; Teubner et al., 2003; Kamarainen et al., 2009). For example, the excretion of inorganic phosphorus by zooplankton alone can potentially account for a significant fraction of the phosphorus supply to the mixed layer in a wide range of morphologically and geographically diverse lakes (Gulati et al., 1995; Arhonditsis et al., 2004a; Kowalezewska-Madura et al., 2007). Likewise, Goldman (1984) has described the intense microbially mediated recycling as a rapidly turning "spinning wheel", whereby nutrients are returned into the system in short time scales (<1 day) with minimal losses. Because of their capacity to modulate the autotrophic activity, existing research efforts have primarily focused on different facets of the nitrogen and phosphorus cycling.

Aside from an indispensable pathway for understanding the ecosystem functioning, the "microbial loop" represents an important agent of nutrient cycling (Azam et al., 1983). Namely,

* Corresponding author. Tel.: +1 416 208 4858; fax: +1 416 287 7279.
E-mail address: georgea@utsc.utoronto.ca (G.B. Arhonditsis).

0304-3800/$ – see front matter © 2012 Elsevier B.V. All rights reserved.
http://dx.doi.org/10.1016/j.ecolmodel.2012.04.018

counter to the historical paradigm that postulated nearly all primary production passing through a linear food chain, our contemporary understanding suggests that a large proportion of autochthonous autotrophic production may be diverted to the microbial community (bacteria, autotrophic picoplankton, heterotrophic nanoflagellates, and ciliates) rather than being transferred directly to higher trophic levels (Kamarainen et al., 2009). As a result, the microbially-mediated regeneration is responsible for considerable subsidies of bioavailable nutrients into the epilimnetic environment, and can therefore introduce strong positive feedback links at the base of the food web (Fasham et al., 1990; Moloney and Field, 1991a,b; Stone and Berman, 1993). The well-documented "boom and bust" phytoplankton cycles are, at least in some cases, modulated by the dynamics of the nutrient fluxes emanating from the microbial loop (Weisse et al., 1990). The microbial food web also appears to shape the oscillatory patterns induced by intermittent nutrient pulses, typically originating from winds, storms, internal waves, and solitons (Stone and Berman, 1993). In an attempt to shed light on the magnitude and frequency of the regeneration of mineral nutrients, Azam et al. (1983) highlighted the importance of several interacting ecological relationships (i.e., commensalism, competition, and predation) among the constituents of the microbial community. Subsequent studies examined the decomposition and mineralization efficacy of individual groups (bacteria, heterotrophic nanoflagellates) against a variety of substrates (e.g., macrophytes, living and/or dead algal cells) with different nutritional/biochemical content (Sherr et al., 1982; De Pinto et al., 1986; Bloem et al., 1989; Berman et al., 1999; Teubner et al., 2003). Generally, the influence of the osmotrophic microbial community on nutrient recycling processes is assumed to be maximal in oligotrophic systems, but the relative role of particle-feeding heterotrophs (protozoa, zooplankton, and fish) appears to concomitantly increase with an increase in ecosystem productivity (Cotner and Biddanda, 2002).

Animals represent another important mediator of nutrient cycling in aquatic ecosystems. Vanni (2002) distinguished between two mechanisms through which animal-mediated cycling can influence ecosystem processes: nutrient recycling and nutrient translocation. The former mechanism depicts the direct release of nutrients from an animal within the same habitat where food was ingested, while the latter refers to the procedure by which animals physically move nutrients between different habitats (e.g., from benthic to pelagic habitats) or even different ecosystems. In this regard, Vanni (2002) contended that the distinct feature of nutrient translocation is that it allows the movement across physical boundaries (e.g., the sediment-water interface, the thermocline that separates surface and deep water layers) or physical processes (e.g., the unidirectional advective flow of water in streams) that impede nutrient availability, and thus can significantly increase the mass of nutrients in a particular habitat. On the other hand, the animal nutrient excretion is an exceptionally effective means to fuel autotrophic productivity, as most of the excreted material is supplied in directly bioavailable inorganic forms (e.g., ammonia, phosphate). Because of allometric constraints on metabolism (Peters, 1983), mass-specific nutrient excretion rates of animals (i.e., nutrients excreted per unit of biomass) usually decrease with increasing body mass, and thus the smallest organisms (e.g., rotifers, protozoa) are being associated with higher rates of phosphorus excretion per unit of biomass relative to the large ones, e.g., cladocerans, copepods (Gulati et al., 1989; Peduzzi and Herndl, 1992; Ejsmont-Karabin et al., 2004; Kowalezewska-Madura et al., 2007). Nutrient excretion rates also increase with temperature due to the dependence of metabolic rates on temperature (Devine and Vanni, 2002). Further, the ratio at which animals excrete the different nutrients (C:N:P) can conceivably shape the type and severity of nutrient limitation (Sterner and Elser, 2002), the composition of algal assemblages (Elser and Urabe, 1999), and the nature of sedimentation fluxes (Elser and Foster, 1998; Arhonditsis and Brett, 2005b).

The intensification and prolongation of lake stratification due to climate warming can presumably magnify the severity of nutrient limitation (Winder and Hunter, 2008; Law et al., 2009), and thus may increase the dependence of planktonic food webs on internal nutrient regeneration mechanisms (Shimoda et al., 2011). Others assert that one of the possible effects of warmer water temperatures may be the increased lake productivity due to enhanced nutrient remineralization (Blenckner et al., 2002), as the associated metabolic/excretion processes can increase by a factor of 1.5–2.5 for every 10 °C temperature increase, i.e., the so-called Q_{10} rule (Vanni, 2002). Our fundamental understanding of nutrient regeneration suggests that the strength of the recycling feedback loop can be indeed related to climate forcing, but the trophic status of a given system along with the associated abiotic conditions and the structure of the biotic communities may be equally important. In this context, some of the critical knowledge gaps involve the strength of the relationship between mineralization rates and lake warming. Considerable uncertainty also exists in regards to the capacity of different metabolic strategies and/or the composition of plankton assemblages to determine the importance of the causal link between climate variability and nutrient regeneration. Our study aims to shed light on these issues using a complex biogeochemical model that simulates multiple elemental cycles (C, N, P, Si, O), multiple functional phytoplankton (diatoms, green algae and cyanobacteria) and zooplankton (copepods and cladocerans) groups. The model provides a realistic means for examining the influence of nutrient regeneration mechanisms on phytoplankton–zooplankton interactions and inter-specific competition patterns, while accounting for the variability in nutrient loading conditions and climatic regimes. The probabilistic treatment of the input vector (e.g., model parameters, forcing functions) of our complex model allows detecting statistically significant trends related to the seasonal variability of plankton biomass or particulate sedimentation fluxes. Our study concludes by identifying some problems of the existing mathematical depictions of the recycling rates, and emphasizes the need to improve our understanding of the interplay among microbial metabolism, trophic states, and lake thermal dynamics.

2. Methods

2.1. Aquatic biogeochemical model

2.1.1. Model description

The spatial structure of the model consists of two compartments, representing the epilimnion (upper layer) and hypolimnion (lower layer) of a hypothetical north-temperate monomictic lake. The model simulates five biogeochemical cycles, i.e., organic carbon, nitrogen, phosphorus, silica and dissolved oxygen (Fig. S1 in Electronic Supplementary Material). The particulate phase of the nutrients is explicitly considered by the state variables for particulate organic carbon (POC), particulate organic nitrogen (PON), particulate organic phosphorus (POP), and particulate silica (PSi). The dissolved phase fractions comprise dissolved organic forms of carbon (DOC), nitrogen (DON), and phosphorus (DOP) and inorganic forms including nitrate (NO_3), ammonium (NH_4), phosphate (PO_4), silica (DSi), and oxygen (DO). The major sources and sinks of the particulate forms include plankton basal metabolism, egestion of excess particulate matter during zooplankton feeding, settling to the hypolimnion or sediment, dissolution of particulate nutrient forms, external loading, and outflow losses. Similar processes govern the levels of the dissolved organic and

inorganic forms along with the mineralization and vertical diffusive transport. The model also explicitly simulates denitrification, nitrification, heterotrophic respiration, and water column-sediment exchanges. The external forcing of the model consists of the river inflows, precipitation, evaporation, solar radiation, water temperature, and nutrient loading. The reference conditions for our analysis correspond to the average epilimnetic/hypolimnetic temperature, solar radiation, vertical diffusive mixing, hydraulic and nutrient loading in Lake Washington (Arhonditsis and Brett, 2005a,b; Brett et al., 2005). Following the Zhao et al. (2008a,b) protocol, the average input nutrient concentrations for the oligo-, meso-, and eutrophic environments correspond to 50 (2.9 mg TOC L^{-1}, 484 μg TN L^{-1} and 32.5 μg TP L^{-1}), 100 (5.8 mg TOC L^{-1}, 967 μg TN L^{-1} and 65 μg TP L^{-1}), and 200% (11.6 mg TOC L^{-1}, 1934 μg TN L^{-1} and 130 μg TP L^{-1}) of the reference conditions, respectively. A detailed model description has been provided elsewhere (Arhonditsis and Brett, 2005a; Zhao et al., 2008a,b), and therefore our focus herein will be on the planktonic parameters associated with the recycling rates and particulate fluxes.

The phytoplankton production and losses are governed by growth, basal metabolism, herbivorous zooplankton grazing, settling to hypolimnion or sediments, epilimnion/hypolimnion diffusion exchanges, and outflow losses. Nutrient, light, and temperature effects on phytoplankton growth are considered using a multiplicative equation (Jorgensen and Bendoricchio, 2001). Our model considers three phytoplankton functional groups (diatoms, green algae, and cyanobacteria) that differ with regards to their strategies for resource competition (i.e., nitrogen, phosphorus, light, temperature) as well as their metabolic rates and morphological features (i.e., settling velocity, self shading effects). Diatoms are modelled as r-selected organisms with high maximum growth rates and higher metabolic losses, superior phosphorus and inferior nitrogen kinetics, lower tolerance to low light availability, lower temperature optima, silica requirements, and high sinking velocities. By contrast, cyanobacteria are modelled as K-strategists with low maximum growth and metabolic rates, higher tolerance to low light availability, low settling velocities, higher temperature optima, slow phosphorus and fast nitrogen kinetics, and higher self shading effects (e.g., filamentous cyanobacteria). The parameterization of the third functional group (labelled as "Green Algae") aimed to provide an intermediate competitor that more realistically depicts the continuum between diatom- and cyanobacteria-dominated communities in our numerical experiments. In addition, the three phytoplankton groups differ in regards to their palatability and food quality for herbivorous zooplankton. Each producer species is parameterized with a minimum internal nutrient requirement, which is the lowest possible intracellular resource concentration required for growth (i.e., minimum nutrient quota). A maximum nutrient bound is also considered to account for the maximum physiological storage (Hamilton and Schladow, 1997). These parameterizations are built upon the different enzymatic reactions taking place across phytoplankton species, resulting in different nutrient affinities and uptake rates depending on both intra- and extra-cellular nutrient concentrations (Zhao et al., 2008a).

The herbivorous zooplankton biomass is controlled by growth, basal metabolism/higher predation, and outflow losses. The zooplankton grazing term explicitly considers the impact of algal food quality on zooplankton assimilation efficiency, and also takes into account recent advances in stoichiometric nutrient recycling theory (Arhonditsis and Brett, 2005a; Zhao et al., 2008b). The zooplankton community of the model consists of two functional groups (cladocerans and copepods) that have different grazing rates, food preferences, selectivity strategies, elemental somatic ratios, vulnerability to predators, and temperature requirements. Cladocerans are modelled as filter-feeders with an equal preference among the four food-types considered in our model (diatoms, green algae, cyanobacteria, and detritus), high maximum grazing rates and metabolic losses, lower half saturation for growth efficiency, higher temperature optima, high sensitivity on low temperatures, low nitrogen and high phosphorus content. By contrast, copepods are characterized by lower maximum grazing and metabolic rates, capability of selecting on the basis of food quality, higher feeding rates at low food abundance, and lower temperature optima with a greater temperature adaptive capacity (Arhonditsis and Brett, 2005a; Zhao et al., 2008b). Seston food quality in the model is dynamically characterized as a function of two factors: (i) the imbalance between the C:P ratio of the grazed seston and a critical $C:P_0$ ratio above which zooplankton growth is limited by P availability; and (ii) the variability in food quality due to differences in highly unsaturated fatty acid, amino acid, protein content and/or digestibility (Zhao et al., 2008b).

Following Mulder and Bowden's (2007) proposition, we have relaxed the assumption of strict zooplankton homeostasis by considering dynamic phosphorus to carbon ratio that varies with the seston phosphorus content and the zooplankton ability to cope with mineral phosphorus limitation:

$$\frac{P}{C_{ZOOP}} = \frac{P}{C_{opt(ZOOP)}} - \left(1 - \frac{P_{seston}}{P/C_{opt(ZOOP)}}\right)^{N} \times \left(\frac{P}{C_{opt(ZOOP)}} - \frac{P}{C_{min(ZOOP)}}\right) \quad (1)$$

where the somatic phosphorus to carbon ratio, P/C_{ZOOP}, is modeled as a function of the parameters $P/C_{opt(ZOOP)}$ and $P/C_{min(ZOOP)}$, representing the zooplankton optimum and minimum phosphorus to carbon ratios; P_{seston} denotes the phosphorus to carbon ratio of the grazed seston; N corresponds to a regulatory coefficient. Thus, according to Eq. (1), zooplankton somatic stoichiometry deviates from its optimal stoichiometry due to the disparity between seston and somatic phosphorus content. The impact of this disparity is further modulated by a regulatory coefficient (N) aiming to represent an organism's homeostatic rigidity; namely, larger N values represent stricter homeostasis (Sterner and Elser, 2002). The regulatory term is also scaled by the difference between optimal and minimum somatic P:C ratios. The inclusion of Eq. (1) in our model allows the zooplankton nutrient use efficiency to vary with food quality (Mulder and Bowden, 2007). Prior to our analysis, we examined the variability of the total phytoplankton biomass induced by the interplay between the three zooplankton stoichiometric properties, i.e., zooplankton optimum (P/C_{opt}) and minimum (P/C_{min}) phosphorus to carbon ratios, and the regulatory coefficient (N), against a wide range of exogenous nutrient loading conditions (Fig. S2). Our modeling experiment highlighted the capacity of both the optimum and minimum P:C somatic ratios to modulate the slope of the TP–phytoplankton relationship. In particular, the phytoplankton response to ambient TP levels becomes significantly more pronounced, when we assume $P/C_{min(ZOOP)}$ and $P/C_{opt(ZOOP)}$ values higher than 0.01 and 0.03 mg P/mg C. On the other hand, the changes of the regulatory coefficient N exert minimal control on the phytoplankton biomass levels for any given TP concentration with the present model structure and parameterization.

2.1.2. Model application

Our Monte Carlo analysis examines the role of plankton stoichiometric properties, the parameters associated with the nutrient recycling rates, and abiotic conditions (e.g., temperature, nutrient loading) on the planktonic food web patterns in oligo-, meso-, and eutrophic environments (Fig. 1). We assigned normal probability distributions that reflect our knowledge from field observations, laboratory studies, literature information, and expert judgment

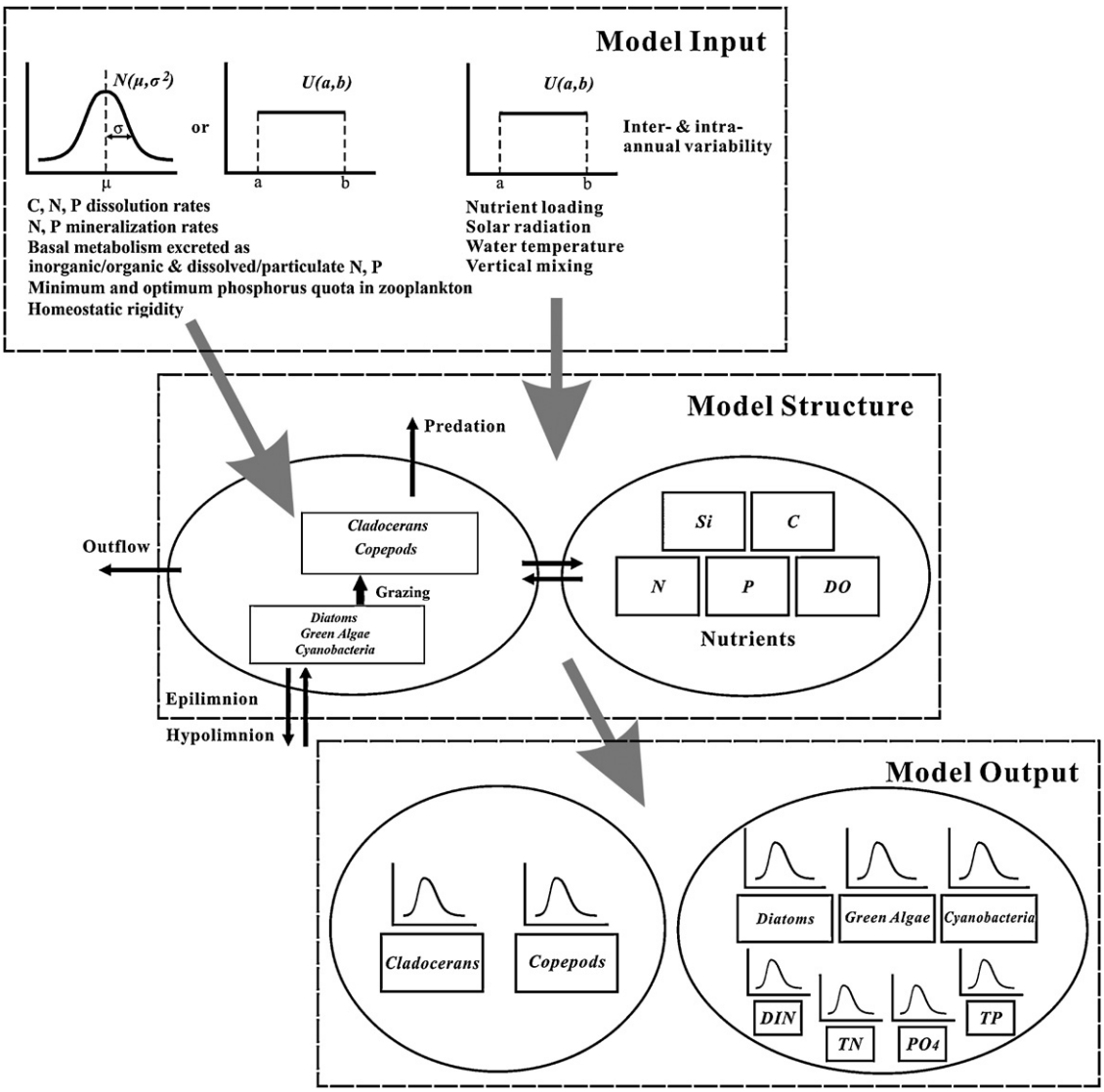

Fig. 1. Monte Carlo analysis of the aquatic biogeochemical model. The input vector consists of parameters related to nutrient regeneration mechanisms (dissociation and mineralization rates, fractions of the plankton metabolism and food egested recycled into the system as particulate or dissolved phase carbon, nitrogen and phosphorus) and zooplankton stoichiometric properties (zooplankton minimum and phosphorus somatic content, homeostatic rigidity) as well as forcing functions (nutrient loading, solar radiation, water temperature, and vertical diffusive mixing).

Table 1
Monte Carlo analysis – definitions and statistical distributions of the model parameters examined.

Model parameter	Symbol	Unit measurement	Phytoplankton	Zooplankton	Sources
Effects of temperature on planktonic metabolic processes	$KT_{planktonicref}$	$^{\circ}C^{-2}$	U(0.001, 0.01)	U(0.001, 0.01)	4
Particulate carbon dissolution rate at reference temperature	$K_{dissolc\text{-}ref}$	day^{-1}	$N(0.01, 0.02^2)$	$N(0.01, 0.02^2)$	1
Particulate nitrogen dissolution rate at reference temperature	$K_{dissoln\text{-}ref}$	day^{-1}	$N(0.01, 0.02^2)$	$N(0.01, 0.02^2)$	1
Particulate phosphorus dissolution rate at reference temperature	$K_{dissolp\text{-}ref}$	day^{-1}	$N(0.01, 0.02^2)$	$N(0.01, 0.02^2)$	1
Phosphorus mineralization rate at reference temperature	$K_{mineralp\text{-}ref}$	day^{-1}	$N(0.035, 0.105^2)$	$N(0.035, 0.105^2)$	1,2,3
Nitrogen mineralization rate at reference temperature	$K_{mineraln\text{-}ref}$	day^{-1}	$N(0.012, 0.022^2)$	$N(0.012, 0.02^2)$	1,2
Fraction of basal metabolism excreted as DOP	FBM_{DOP}	–	U(0.05, 0.30)	U(0.05, 0.30)	1
Fraction of basal metabolism excreted as DON	FBM_{DON}	–	U(0.05, 0.30)	U(0.05, 0.30)	1
Fraction of basal metabolism excreted as DOC	FBM_{DOC}	–	U(0.05, 0.30)	U(0.05, 0.30)	1
Fraction of basal metabolism excreted as phosphate	FBM_{PO4}	–	U(0.05, 0.50)	U(0.05, 0.50)	1
Fraction of basal metabolism excreted as ammonium	FBM_{NH4}	–	U(0.05, 0.50)	U(0.05, 0.50)	1
Fraction of DOP egested during zooplankton feeding	FE_{DOP}	–	U(0.05, 0.30)	U(0.05, 0.30)	1
Fraction of DON egested during zooplankton feeding	FE_{DON}	–	U(0.05, 0.30)	U(0.05, 0.30)	1
Fraction of DOC egested during zooplankton feeding	FE_{DOC}	–	U(0.05, 0.30)	U(0.05, 0.30)	1
Fraction of phosphate egested in zooplankton feeding	FE_{PO4}	–	U(0.05, 0.50)	U(0.05, 0.50)	1
Fraction of ammonium egested in zooplankton feeding	FE_{NH4}	–	U(0.05, 0.50)	U(0.05, 0.50)	1
Optimum zooplankton phosphorus to carbon ratio	$P/C_{opt(ZOOP)}$	mg P mg C^{-1}		U(0.020, 0.035)	4
Minimum zooplankton phosphorus to carbon ratio	$P/C_{min(ZOOP)}$	mg P mg C^{-1}		U(0.004, 0.014)	4
Regulatory coefficient	N	–		U(1.0, 3.0)	4

(1) Cerco and Cole (1994) and references therein; (2) Hamilton and Schladow (1997) and references therein; (3) Omlin et al. (2001); (4) Mulder and Bowden (2007).

on the relative plausibility of the dissociation and mineralization rates. Uniform distributions were also assigned to accommodate the uncertainty associated with the fractions of the plankton metabolism and food egested that were returned back into the system as particulate or dissolved phase carbon, nitrogen and phosphorus. In addition, ±20% perturbations have been induced to accommodate the intra- and inter annual variability associated with the solar radiation, water temperate, vertical mixing, and external nutrient loading in a typical north-temperate system. All definitions and statistical distributions assigned to the corresponding parameters are presented in Table 1. For each trophic state, we generated 7000 input vectors independently sampled from 58 probability distributions (i.e., 53 model parameters and 5 forcing functions), which were then used to run the model for 10 years. Finally, we generated matrices (7000×12) that comprised the average monthly epilimnetic values for total phytoplankton and zooplankton biomass, particulate carbon, nitrogen, and phosphorus fluxes, total nitrogen (TN), nitrate (NO_3), ammonium (NH_4), phosphate (PO_4), and total phosphorus (TP) concentrations in each trophic states.

2.2. Statistical methodology

2.2.1. Principal component analysis and multiple linear regression models

Principal component analysis (PCA), a data reduction and structure detection technique (Legendre and Legendre, 1998), was applied to identify different seasonal modes of intra-annual variability (Jassby, 1999; Arhonditsis et al., 2004a,b). The basic rationale behind this PCA application is that different phases of the intra-annual cycle may be regulated by distinct mechanisms and may therefore behave independently of each other, thereby impeding identification of clear cause–effect relationships (Jassby, 1999). In each trophic state, for total phytoplankton and zooplankton biomass, the particulate carbon, nitrogen and phosphorus fluxes, we used PCA with the aforementioned matrices to unravel the number of independent seasonal modes of biomass variability, and the months of year in which they were most important (component coefficients). Principal components (PCs) were estimated by singular value decomposition of the covariance matrix of the Monte Carlo outputs. The selection of significant PCs was based on the Kaiser criterion, i.e., we retained only PCs with eigenvalues greater than 1. The significant seasonal modes were rotated using the normalized varimax strategy to calculate the new component coefficients (Richman, 1986). We then developed multiple linear regression models within the resultant seasonal modes of variability. When a pair response variable-trophic state did not result in the extraction of significant PCs, the multiple regression analysis was conducted for each month. The multiple regression analysis intended to identify the basic mechanisms that underlie the seasonal modes of total phytoplankton biomass, zooplankton biomass, and the particulate fluxes of carbon, nitrogen and phosphorus variability. We used plankton stoichiometric properties, nutrient recycling parameters, and the abiotic conditions considered in our Monte Carlo analysis as predictor variables. In each model, we reported the five most significant predictors, based on the absolute value of the standardized regression coefficients ($|\beta|$).

3. Results

3.1. Summary statistics of the Monte Carlo analysis

Table 2 provides the summary statistics of the major limnological variables across the three trophic states, as derived from the model outputs averaged over the 10-year simulation period. The

Table 2
Monte Carlo analysis of the aquatic biogeochemical model across three trophic states: summary statistics of the mean annual values of the phosphate (PO_4), total phosphorus (TP), dissolved inorganic nitrogen (DIN), total nitrogen (TN), the ratio of total nitrogen to total phosphorus (TN:TP), diatom biomass (DB), green algae biomass (GB), cyanobacteria biomass (CYB), cladoceran biomass (CLB), copepod biomass (COB), particulate carbon flux (PCF), particulate nitrogen flux (PNF), and particulate phosphorus flux (PPF).

	PO_4 ($\mu g L^{-1}$)	TP ($\mu g L^{-1}$)	DIN ($\mu g L^{-1}$)	TN ($\mu g L^{-1}$)	TN/TP	DB (μg Chla L^{-1})	GB (μg Chla L^{-1})	CYB (μg Chla L^{-1})	CLB (μg C L^{-1})	COB (μg C L^{-1})	PCF (mg m^{-2} day^{-1})	PNF (mg m^{-2} day^{-1})	PPF (mg m^{-2} day^{-1})
Oligotrophic													
Mean	5.6	11.0	223	313	29.0	1.3	0.8	0.4	24.9	19.8	96.2	13.1	1.6
Median	5.5	10.9	223	311	28.8	1.3	0.8	0.4	24.7	19.5	96.0	12.9	1.6
Range	3–9	6–21	155–285	235–450	15–47	1–2	0.3–1	0.01–0.8	10–43	8–36	65–141	6–24	1–2
Mesotrophic													
Mean	8.4	17.1	261	396	23.6	1.5	1.0	0.7	39.3	34.6	126	15.6	2.0
Median	8.3	16.8	261	391	23.5	1.5	1.0	0.7	38.9	34.1	125	15.4	2.2
Range	5–14	11–31	169–347	300–602	13–40	1–2	0.7–1	0.4–1.2	23–64	19–58	99–172	5–28	1–2
Eutrophic													
Mean	14.9	29.4	353	555	19.5	1.7	1.3	1.3	63.1	60.5	163	17.5	2.9
Median	14.9	29.6	350	554	19.2	1.7	1.3	1.3	62.7	60.0	162	17.2	2.9
Range	7–29	17–49	233–497	378–635	11–30	1.4–2	0.9–2	1–2	36–102	33–93	128–205	2–35	2–3

corresponding seasonal variability is illustrated in Figs S3–S6 (Electronic Supplementary Material). Generally, the variability induced by the parameters associated with the nutrient recycling rates and the zooplankton stoichiometric properties as well as the forcing functions examined was comparable to what has been reported in our earlier work with other important plankton food web processes, e.g., growth rates, nutrient kinetics, metabolic strategies, and higher predation rates (Zhao et al., 2008a,b). The average annual phosphate (PO_4) and total phosphorus (TP) concentrations dramatically increased by nearly 250% from the oligotrophic to the eutrophic environment, while the corresponding dissolved inorganic nitrogen (DIN) and total nitrogen (TN) increases were lower ($\leq$83%). The ratio of total nitrogen to total phosphorus (TN:TP) supported stoichiometric predictions of phosphorus limitation in the three states. The transition from an oligotrophic to eutrophic environment was associated with the relaxation of the phosphorus limitation though, as TN:TP declined from 29.0 to 19.5. While several Monte Carlo simulations depicted nitrogen-limiting conditions (TN:TP < 16:1), it should be noted that similar conclusions are not fully supported if we compare the ambient PO_4 and DIN levels relative to the phytoplankton half saturation constant values assigned to nitrogen and phosphorus uptake (see Appendix B in Arhonditsis and Brett, 2005a).

The biomass of the three phytoplankton functional groups showed an increasing trend in response to the nutrient enrichment. Phosphorus availability determined the success of the different phytoplankton functional groups. Diatoms posses superior phosphorus kinetics and therefore consistently dominated the phytoplankton community. Yet, their abundance was moderately increased, from 1.3 to 1.7 μg chla L^{-1}, following the nutrient enrichment of the system. Being the intermediate competitors, green algae demonstrated less than twofold increase, shifting from oligotrophic (0.8 μg chla L^{-1}) to the eutrophic state (1.3 μg chla L^{-1}). Cyanobacteria, the weakest phosphorus competitors, represented a relatively low proportion of the total phytoplankton biomass in the oligotrophic environment (0.4 μg chla L^{-1}). However, the cyanobacteria handicap for phosphorus was alleviated in the eutrophic environment and their mean biomass increased by more than 300% ($\sim$1.3 μg chla L^{-1}). In response to the algal biomass increase, the biomass of the two zooplankton groups gradually increased across the three trophic states, i.e., both cladocerans and copepods demonstrated more than twofold (from 24.9 to 63.1 μg C L^{-1}) and threefold (from 19.8 to 60.5 μg C L^{-1}) increases, respectively. The average annual particulate fluxes also increased across the three trophic states. Namely, the particulate carbon flux increased from 96.2 to 163 mg m^{-2} day^{-1}, while the particulate nitrogen flux increased from 13.1 to 17.5 mg m^{-2} day^{-1}. Likewise, the particulate phosphorus sedimentation demonstrated a nearly twofold increase (i.e., from 1.6 to 2.9 mg m^{-2} day^{-1}). Moreover, the increase in the particulate nitrogen and phosphorus fluxes closely followed the seasonal patterns of autochthonous production, which was characterized by a spring peak associated with the concurrent phytoplankton bloom as well as a mid/late summer secondary peak that became more pronounced in the meso- and eutrophic environments (Fig. S6).

3.2. Principal component analysis and multiple linear regression models

3.2.1. Seasonal phytoplankton patterns

The PCA revealed the existence of two distinct seasonal modes of phytoplankton variability in the oligotrophic environment (Fig. S7, Table 3). The first seasonal mode represented the mid/late spring (April, May) along with the summer stratified period until the end of calendar year (August–December). The second mode represented the period when the lake was vertically homogeneous (January–March) and the early summer (June). The total phytoplankton biomass patterns in the mesotrophic environment were also characterized by two seasonal modes. The first seasonal mode represented the summer stratified, the fall turnover and most of the winter period (July–January), whereas the second seasonal mode of variability covered the rest of the winter (February, March) and the late spring/early summer (June). In the eutrophic environment, three modes of seasonal variability were extracted. The first seasonal mode covered the winter months (January–March), mid/late spring (May, June), and the end of summer (August). The second mode was characterized by the fall turnover (October–December), while the months of July and September formed the third seasonal mode. We also highlight the strongly negative component coefficients associated with the end of spring mean phytoplankton values in the meso- and eutrophic settings.

The epilimnetic temperature ($Temperature_{epi}$) was the most influential factor ($\approx|\beta| > 0.60$) of the total phytoplankton variability during the first and second seasonal modes in all three trophic environments. Epilimnetic temperature had a consistently negative association with phytoplankton biomass during the first seasonal mode in both oligo- and mesotrophic environments. On the other hand, the same negative relationship was manifested during the second mode of seasonal phytoplankton variability under higher nutrient enrichment conditions (eutrophic state). Interestingly, hypolimnetic temperature ($Temperature_{hypo}$) was also among the five most influential parameters during the seasonal modes associated with the winter months in all trophic states, although this causal linkage had the opposite sign (negative) relative to the concurrent relationship between epilimnetic temperature and phytoplankton (Table 3). This somewhat counterintuitive relationship probably reflects the negative association between net hypolimnetic phytoplankton growth (light-limited growth minus basal metabolism) and water temperature, which subsequently generates vertical phytoplankton gradients and thus diffusive mass exchanges between epilimnion and hypolimnion. The external nutrient loading was another significant factor positively related to the total phytoplankton biomass in both oligo- and mesotrophic environments ($|\beta| > 0.28$). Notably, the signature of nutrient loading variability on phytoplankton dynamics disappeared under the eutrophic conditions. The total phytoplankton biomass levels were also dependent on the fraction of basal metabolism of diatoms excreted as phosphate, $FBM_{PO4}(D)$, in the oligo- and mesotrophic environments. The fraction of phosphate egested during zooplankton feeding, $FE_{PO4}(CL)/(CO)$, was another parameter that appears to modulate phytoplankton dynamics in all trophic environments. Further, the optimal somatic phosphorus to carbon ratio for cladocerans, $P/C_{opt}(CL)$, was one of the critical parameters in the mesotrophic conditions ($|\beta| = 0.24$). Our analysis also reveals that the vertical diffusive mass exchanges exert negative control on the levels of epilimnetic phytoplankton biomass during the seasonal modes associated with the cold months of the year ($\approx|\beta| > 0.18$), although we also note the positive causal link between the same process and epilimnetic phytoplankton ($|\beta| = 0.326$) in the eutrophic state during the third temporal mode, i.e. July and September. Regarding the latter combination of trophic state and time of the year, our analysis showed a negative relationship between the amounts of DOC egested during zooplankton feeding, $FE_{DOC}(CL)$, and the total phytoplankton biomass, suggesting higher allocation of egested carbon to the dissolved-phase fraction and thus distinctly lower levels of particulate matter, which in turn result in lower zooplankton and subsequently higher phytoplankton biomass.

3.2.2. Seasonal zooplankton patterns

Two distinct seasonal modes of zooplankton variability were consistently extracted with the three nutrient loading scenarios

Table 3
Multiple regression models developed for identifying the most influential factors (stoichiometric properties, nutrient recycling parameters and abiotic conditions) associated with total phytoplankton biomass across the three trophic environments examined.

Oligotrophic			
First mode (r^2 = 0.977)	$\|\beta\|$	Second mode (r^2 = 0.966)	$\|\beta\|$
$Temperature_{epi}$[a]	0.633	$Temperature_{epi}$	0.627
$FBM_{PO4}(D)$	0.409	Loading	0.326
Loading	0.311	$FBM_{PO4}(D)$	0.292
$FBM_{DOP}(D)$	0.215	$Temperature_{hypo}$[a]	0.271
$FBM_{PO4}(G)$	0.184	Diffusion[a]	0.202

Mesotrophic			
First mode (r^2 = 0.960)	$\|\beta\|$	Second mode (r^2 = 0.957)	$\|\beta\|$
$FBM_{PO4}(D)$	0.445	$Temperature_{epi}$	0.868
$Temperature_{epi}$[a]	0.307	$Temperature_{hypo}$[a]	0.230
$FE_{PO4}(CL)$	0.298	Diffusion[a]	0.182
Loading	0.288	$K_{mineralp\text{-}ref}$	0.145
$P/C_{opt}(CL)$	0.246	$FE_{PO4}(CO)$	0.118

Eutrophic					
First mode (r^2 = 0.961)	$\|\beta\|$	Second mode (r^2 = 0.953)	$\|\beta\|$	Third mode (r^2 = 0.630)	$\|\beta\|$
$Temperature_{epi}$	0.745	$Temperature_{epi}$[a]	0.589	Diffusion	0.326
$Temperature_{hypo}$[a]	0.342	$FE_{PO4}(CO)$	0.289	$Temperature_{hypo}$	0.282
Diffusion[a]	0.246	$FE_{PO4}(CL)$	0.281	$FE_{PO4}(CL)$	0.260
$FE_{PO4}(CO)$	0.230	$K_{mineralp\text{-}ref}$	0.276	$FE_{DOC}(CL)$[a]	0.251
$K_{mineralp\text{-}ref}$	0.217	$FBM_{PO4}(D)$	0.262	$Temperature_{epi}$	0.218

Symbol $|\beta|$ denotes the absolute value of the standardized regression coefficients.
[a] Negative sign of the standardized regression coefficients.
Oligotrophic environment: First mode: Apr, May, Aug–Dec; Second mode: Jan–Mar, Jun.
Mesotrophic environment: First mode: Jan, Apr, Jul–Dec; Second mode: Feb, Mar, May[b], Jun.
Eutrophic environment: First mode: Jan–Mar, May[b], Jun, Aug; Second mode: Oct–Dec; Third mode: Jul, Sep.
[b]Component coefficients with negative sign.

(Table 4 and Fig. S8). The first seasonal mode spanned the period from May to December and the second one extended from January to April. We also note that the average zooplankton biomass values in June were characterized by distinctly negative component loading values on the latter seasonal mode in the meso- and eutrophic settings. The epilimnetic temperature ($Temperature_{epi}$) was negatively ($|\beta| > 0.48$) and positively ($|\beta| > 0.61$) related to the total zooplankton biomass in all trophic environments during the

Table 4
Multiple regression models developed for identifying the most influential factors (stoichiometric properties, nutrient recycling parameters and abiotic conditions) associated with total zooplankton biomass across the three trophic environments examined.

Oligotrophic			
First mode (r^2 = 0.976)	$\|\beta\|$	Second mode (r^2 = 0.981)	$\|\beta\|$
$Temperature_{epi}$[a]	0.654	Loading	0.626
$FBM_{PO4}(D)$	0.355	$Temperature_{epi}$	0.611
Loading	0.292	$FBM_{PO4}(D)$	0.226
$FBM_{DOP}(D)$	0.191	$Temperature_{hypo}$[a]	0.198
$P/C_{opt}(CL)$	0.188	Diffusion[a]	0.155

Mesotrophic			
First mode (r^2 = 0.964)	$\|\beta\|$	Second mode (r^2 = 0.977)	$\|\beta\|$
$Temperature_{epi}$[a]	0.534	$Temperature_{epi}$	0.697
$FBM_{PO4}(D)$	0.343	Loading	0.453
Loading	0.279	$Temperature_{hypo}$[a]	0.225
$FE_{PO4}(CL)$	0.257	$P/C_{opt}(CO)$	0.195
$P/C_{opt}(CL)$	0.252	$K_{dissolc\text{-}ref}$[a]	0.187

Eutrophic			
First mode (r^2 = 0.966)	$\|\beta\|$	Second mode (r^2 = 0.963)	$\|\beta\|$
$Temperature_{epi}$[a]	0.486	$Temperature_{epi}$	0.676
$FE_{PO4}(CL)$	0.315	$P/C_{opt}(CO)$	0.384
$K_{mineralp\text{-}ref}$	0.309	Loading	0.282
$P/C_{opt}(CL)$	0.307	$FE_{DOC}(CO)$[a]	0.261
$FBM_{PO4}(D)$	0.260	$Temperature_{hypo}$[a]	0.255

Symbol $|\beta|$ denotes the absolute value of the standardized regression coefficients.
[a] Negative sign of the standardized regression coefficients.
Oligotrophic environment: First mode: May–Dec; Second mode: Jan–Apr.
Mesotrophic environment: First mode: May–Dec; Second mode: Jan–Apr, Jun[b].
Eutrophic environment: First mode: May–Dec. Second mode: Jan–Apr, Jun[b].
[b]Component coefficients with negative sign.

Table 5
Multiple regression models developed for identifying the most influential factors (stoichiometric properties, nutrient recycling parameters and abiotic conditions) associated with particulate carbon fluxes across the three trophic states.

Oligotrophic

First mode (r^2 = 0.979)	$\|\beta\|$	Second mode (r^2 = 0.960)	$\|\beta\|$
$Temperature_{epi}$	0.646	$FBM_{PO4}(D)$	0.399
Loading	0.610	$Temperature_{epi}$[a]	0.390
$K_{dissolc\text{-}ref}$[a]	0.223	$FE_{DOC}(CL)$[a]	0.355
$FBM_{DOC}(D)$[a]	0.197	$P/C_{opt}(CL)$	0.263
$P/C_{opt}(CO)$	0.154	$FE_{PO4}(CL)$	0.223

Mesotrophic

First mode (r^2 = 0.963)	$\|\beta\|$	Second mode (r^2 = 0.960)	$\|\beta\|$
$Temperature_{epi}$	0.690	$Temperature_{epi}$[a]	0.509
Loading	0.316	$FBM_{PO4}(D)$	0.326
$K_{dissolc\text{-}ref}$[a]	0.267	$FE_{DOC}(CL)$[a]	0.324
$P/C_{opt}(CO)$	0.256	$P/C_{opt}(CL)$	0.305
$FE_{DOC}(CO)$[a]	0.199	$FE_{PO4}(CL)$	0.222

Eutrophic

First mode (r^2 = 0.918)	$\|\beta\|$	Second mode (r^2 = 0.940)	$\|\beta\|$	Third mode (r^2 = 0.924)	$\|\beta\|$
$P/C_{opt}(CO)$	0.574	$Temperature_{epi}$[a]	0.775	$Temperature_{epi}$	0.441
$FE_{DOC}(CO)$[a]	0.386	$P/C_{opt}(CL)$	0.249	$FE_{DOC}(CL)$[a]	0.440
$Temperature_{epi}$	0.369	$FE_{DOC}(CL)$[a]	0.223	$P/C_{opt}(CL)$	0.324
$K_{dissolc\text{-}ref}$[a]	0.310	$K_{dissolc\text{-}ref}$[a]	0.187	$FE_{PO4}(CL)$	0.301
Loading	0.241	$P/C_{opt}(CO)$	0.177	$K_{dissolp\text{-}ref}$[a]	0.285

Symbol $|\beta|$ denotes the absolute value of the standardized regression coefficients.
[a] Negative sign of the standardized regression coefficients.
Oligotrophic environment: First mode: Jan–Apr, Dec; Second mode: May–Nov.
Mesotrophic environment: First mode: Jan–Apr, Jul–Sep, Dec; Second mode: May, Oct–Nov.
Eutrophic environment: First mode: Jan–Apr, Dec; Second mode: May, Nov, Jun[b]; Third mode: Jun–Oct.
[b] Component coefficients with negative sign.

first and second seasonal modes, respectively. In a manner similar to the phytoplankton biomass, our analysis suggests a negative association between hypolimnetic temperature ($Temperature_{hypo}$) and total zooplankton biomass during the cooler period of the year. Higher values of the fraction released in the form of phosphate from diatom basal metabolism, $FBM_{PO4}(D)$, or egested during cladoceran feeding, $FE_{PO4}(CL)$, as well as higher optimal phosphorus to carbon ratios in cladocerans, $P/C_{opt(CL)}$, have a consistently positive impact to the zooplankton biomass levels, especially during the first seasonal mode. The exogenous nutrient loading was also considered to be one of the most significant factors modulating total zooplankton biomass variability through the control exerted on phytoplankton. The particulate carbon dissolution/hydrolysis rate ($K_{dissolc\text{-}ref}$) and the fraction of dissolved organic carbon egested during copepod feeding, $FE_{DOC}(CO)$, were negatively related to the winter zooplankton biomass values ($|\beta| = 0.18$), whereas a positive linkage exists between phosphorus mineralization rate ($K_{mineralp\text{-}ref}$) and total zooplankton biomass ($|\beta| = 0.31$) in the eutrophic environment during the first mode of temporal variability.

3.2.3. Seasonal sedimentation patterns

Two distinct seasonal modes of variability for particulate carbon fluxes were derived by the PCA application in the oligo- and mesotrophic environments (Table 5 and Fig. S9). Generally, the first seasonal mode mainly represented the winter until mid-spring period (December to April), while the mid/late spring and fall (May and October–November) mainly formed the second seasonal mode of variability. The main difference between oligo- and mesotrophic conditions was the classification of the summer stratified period (July–September) with the second and first seasonal mode, respectively. Our analysis also extracted three distinct seasonal modes of variability associated with the particulate carbon fluxes in the eutrophic environment. The first seasonal mode clearly depicted the cold period of the year when the lake is vertically homogeneous (December–April), the second mode was strongly associated with the variability of particulate carbon fluxes in May and November, while the third seasonal mode represented the summer stratified period until the fall water turnover. Notably, the average carbon sedimentation in June had equally strong component loadings, but with opposite signs, on the second and third mode of variability.

The epilimnetic temperature ($Temperature_{epi}$) was one of the most influential factors that affected the variability of carbon particulate fluxes in the three trophic states, characterized by a positive relationship during the cooler (December–April) and warmer (June–September) periods of the seasonal cycle and a negative one during the seasonal modes predominantly driven by the sedimentation fluxes in May and mid-fall. The fraction of diatom basal metabolism excreted as phosphate, $FBM_{PO4}(D)$, appears to exert positive control on the carbon sedimentation fluxes during the second mode of variability in the oligo- and mesotrophic conditions. The same positive causal association was also manifested between the optimal phosphorus to carbon ratio of the two zooplankton functional groups, $P/C_{opt}(CL)/(CO)$, and the particulate carbon fluxes in all three trophic states. A distinctly negative causal link also exists with the fraction of egested dissolved organic carbon during zooplankton feeding, $FE_{DOC}(CL)/(CO)$. Likewise, the particulate carbon dissolution/hydrolysis rate ($K_{dissolc\text{-}ref}$) was another factor that had a (plausibly) negative impact to the particulate carbon sedimentation in all three trophic environments. Interestingly, the latter parameter was replaced by its phosphorus counterpart ($K_{dissolp\text{-}ref}$), during the summer stratified period in the eutrophic environment.

We also examined the most influential factors associated with particulate nitrogen and phosphorus sedimentation (Tables S1–2).

In cases where the PCA application did not identify more than one significant mode of variability of the nitrogen and phosphorus particulate fluxes, we developed multiple regression models for the individual months. Generally, the most influential factors in nearly all the seasonal modes across all trophic states were the fractions of diatom basal metabolism and zooplankton feeding released/egested as NH_4 and DON with negative impacts on the variability of nitrogen fluxes. In a similar manner, the phosphorous counterparts of the same processes along with the epilimnetic temperature and the exogenous nutrient loading were the most influential factors shaping the variability of particulate phosphorus fluxes.

3.3. Interplay among exogenous loading, nutrient regeneration rates, and climate warming

In the next phase of our analysis, we examined the relative control of nutrient regeneration rates on the total phytoplankton abundance and community composition under different nutrient enrichment and climate forcing regimes. Similar to our Monte Carlo analysis, three distinct phosphorous loading scenarios were implemented to reproduce oligo-, meso- and eutrophic conditions, while the rest parameters were kept as in the calibration vector reported in the Lake Washington application (Arhonditsis and Brett, 2005a, Appendix B). Further, the unimodal response introduced by Arhonditsis and Brett (2005a) was replaced by a piecewise monotonic temperature-cyanobacterial growth relationship to entertain the competitive advantage of cyanobacteria at warmer temperatures. Based on the findings of recent work (Shimoda et al., 2011), the coefficient that represents the control exerted on the cyanobacteria growth rates at high water temperatures (>20 °C) was set equal to 0.20 $°C^{-2}$, while the temperature effects on diatoms and green algae growth were described by the same piecewise monotonic approach with values set at 0.004 and 0.005, respectively (Arhonditsis and Brett, 2005a, Appendix B). To explicitly accommodate the effects of climate warming on the thermal properties, the present average epilimnetic (14 °C) and hypolimnetic (10 °C) temperatures were increased by 2 °C and 1 °C with the warming scenario, respectively. Consistent with empirical and modeling evidence (Arhonditsis et al., 2004b; Coats et al., 2006), the climate warming was assumed to advance the stratification timing by approximately 20 days relative to the present conditions (June 16), coinciding with a decrease of the vertical diffusive mixing by approximately 15%. We then created a variety of nitrogen and phosphorous recycling conditions, spanning the 0.005–0.05 day^{-1} range for the dissolution and mineralization rates with an increment of 0.001 day^{-1}. The model was run for a 10-year period with each of the six trophic state-climate regime combinations, which was a sufficient simulation period to reach an equilibrium phase, i.e., the same pattern was repeated each year. We subsequently recorded phytoplankton abundance and community composition at an arbitrarily chosen day during the summer stratified period (7th, August) of the tenth year.

Our numerical expOur numerical experiments highlighted the role of phosphorus recycling rates as a primary regulatory factor of the phytoplankton abundance and community composition in the oligotrophic and mesotrophic environments. In particular, for a given level of nitrogen dissolution/mineralization, elevated phosphorous regeneration rates can significantly increase the total phytoplankton biomass (Figs. 2a and c), promote the abundance of the weak phosphorus competitors, e.g., cyanobacteria (Figs. 3a and c), and decrease the relative proportion of diatoms (Figs. 4a and c). Given that both our oligo- and mesotrophic scenarios represent phosphorus-limiting conditions, the model plausibly predicts a minimal impact of the nitrogen dissolution/mineralization rates on phytoplankton productivity and community composition. However, under the eutrophic setting, our analysis pinpoints the interplay between nitrogen and phosphorous recycling rates that modulates both phytoplankton biomass and community composition. Conditions of low nitrogen and high phosphorous recycling rates can amplify phytoplankton growth (Fig. 2e) and promote cyanobacteria dominance (Fig. 3e). On the other hand, diatoms are parameterized as weak competitors for nitrogen, and thus higher nitrogen recycling rates alleviate the effects of the nitrogen-limiting conditions prevailing in our simulated eutrophic environment (Fig. 4e).

Our analysis generally suggest that warming temperatures have increased the levels of total phytoplankton biomass and can potentially favour cyanobacteria dominance, but the ecological ramifications of the elevated water temperature are predominantly controlled by the contemporaneous nutrient enrichment conditions. In particular, the phytoplankton patterns under the warming scenario remained practically unaltered in the oligotrophic environment, while the impact of the nutrient recycling rates was fairly similar to our predictions for the present conditions (Figs. 2b–4b). In the mesotrophic setting, our analysis shows that elevated phosphorus recycling rates with warmer water temperatures can trigger algal growth, leading to an increase of the phytoplankton biomass by approximately 1 μg chla L^{-1} along with a 5–8% increase of the cyanobacteria relative abundance (Figs. 2d–4d). By contrast, our modeling experiment with the eutrophic-warming scenario provides evidence of non-monotonic phytoplankton patterns in the two dimensional space explored (Fig. 2f). The significant variability characterizing the aggregated phytoplankton biomass can be explained by the underlying structural shifts of the different functional groups considered. Namely, the region of high P and low N regeneration rates significantly increased the cyanobacteria relative abundance (>60%; Fig. 3f), whereas the shift to higher nitrogen recycling rates diminishes the severity of nitrogen limitation and thus relaxes the competitive handicap of diatoms (Fig. 4f). Finally, the elevated nutrient regeneration rates can potentially magnify plankton dynamics, whereby the amplitude and frequency of population oscillations are significantly increased. Our study illustrates the results of nine combinations of phosphorous and nitrogen dissolution/mineralization rates which reinforce the notion that higher nutrient recycling rates can conceivably induce larger and more frequent algal biomass peaks, especially during the summer stratified period (Fig. 5). Interestingly, the oscillatory behaviour of the system is further accentuated when we force the model with the warming scenario (Fig. 6).

4. Discussion

The upsurge of the microbial loop paradigm has dramatically changed our perception of the aquatic ecosystem functioning (Pomeroy et al., 2007). The idea that the microbial communities constitute a major vector of the flow of mass and energy to the higher trophic levels has sparked an inconceivably wide array of empirical and modeling research. A great deal of the existing efforts aim to delve into the suite of ecological interactions among phytoplankton, bacteria, protozoans and mesozooplankton predators as well as to elucidate processes such as mixotrophy, cannibalism by flagellates, nutrient regeneration in both refractory and non-refractory forms, prey selection, the action of viruses or more complicated nutrient cycling pathways (Capblancq, 1990; Suttle, 1994; Flynn et al., 1996; Vanni et al., 2002; Azam and Malfatti, 2007). Much of this complexity has been portrayed in mathematical models, which in turn have been used for heuristic purposes to advance our theoretical understanding of nutrient recycling and to subsequently generate testable hypotheses (Taylor and Joint, 1990; Davidson, 1996). However, the incorporation of the microbial food

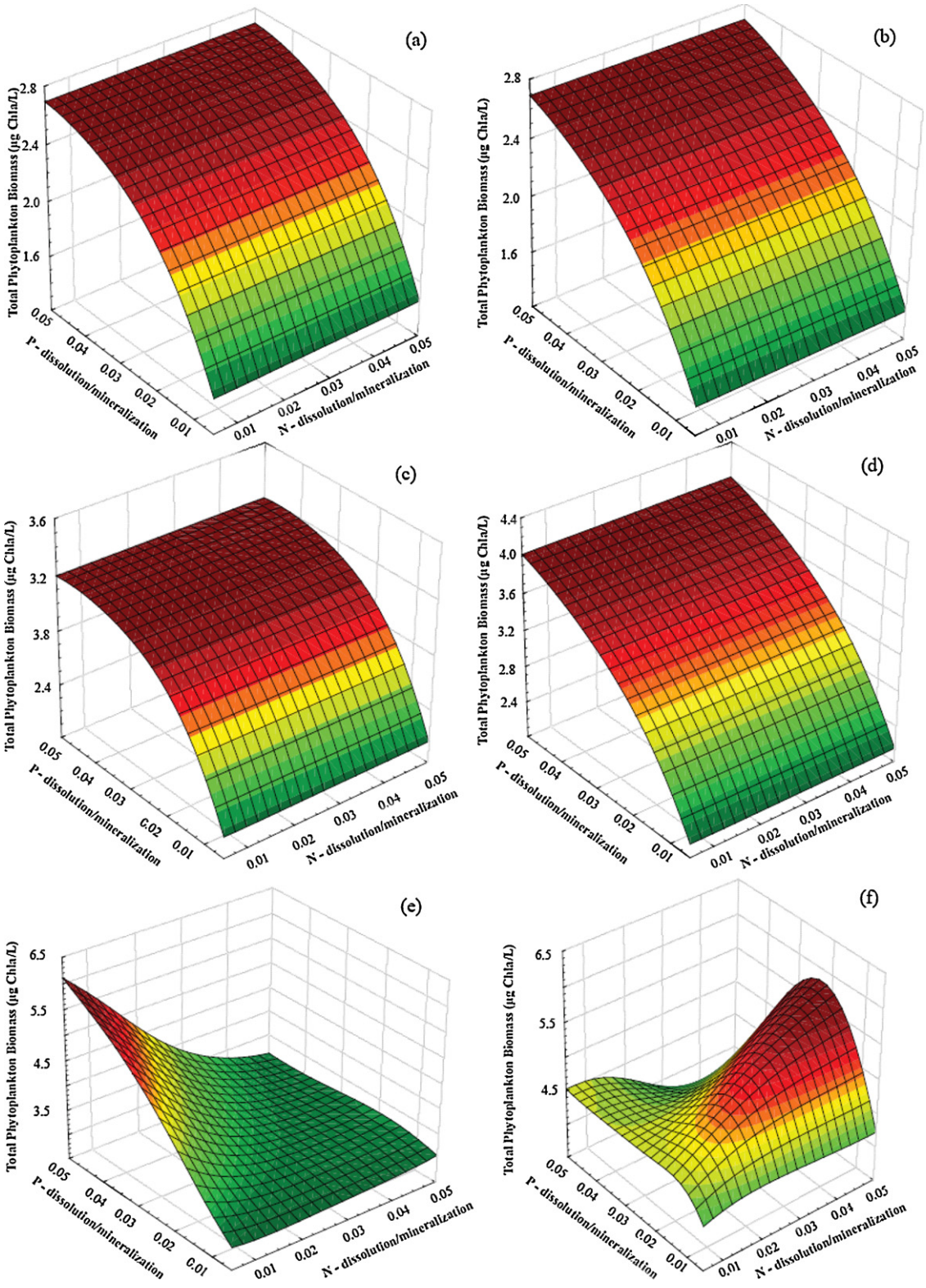

Fig. 2. Total phytoplankton biomass against phosphorus and nitrogen dissolution/mineralization rates in (a,b) oligo-, (c,d) meso-, and (e,f) eutrophic environments. Left panels represent the present water temperature conditions, while the right panels correspond to a warming scenario of approximately +2 °C.

web into management-oriented models is still not commonplace, as the uncertainty underlying the characterization of the associated causal links renders modeling constructs that profoundly violate the parsimony principle and thus undermines their use for predictive purposes (Arhonditsis et al., 2007). Rather, the pragmatic approach typically adopted assumes a constant fraction of the ingested nutrients is returned into the water column in a specific particulate/dissolved or organic/inorganic form as a function of first-order, temperature-dependent, metabolic rates (Jorgensen and Bendoricchio, 2001). While a convenient approximation, this strategy has (inadvertently) shifted the focus of most model parameterization exercises into other aspects of plankton

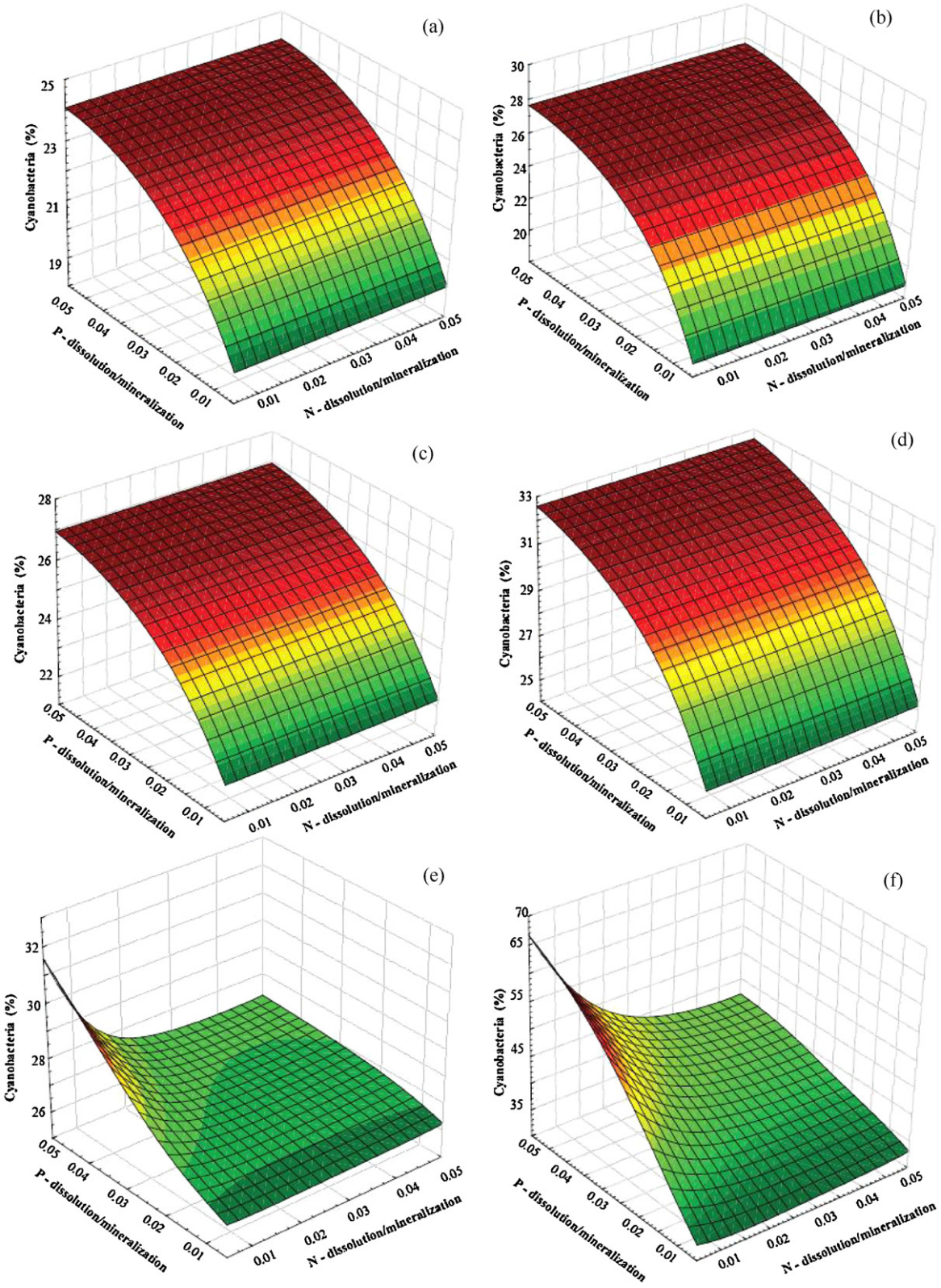

Fig. 3. Cyanobacteria percentage contribution to the total phytoplankton biomass against phosphorus and nitrogen dissolution/mineralization rates in (a,b) oligo-, (c,d) meso-, and (e,f) eutrophic environments. Left panels represent the present water temperature conditions, while the right panels correspond to a warming scenario of approximately +2 °C.

models (e.g., growth and predation rates, nutrient kinetics), and thus downplays the critical role of nutrient recycling in modulating ecosystem response to exogenous loading/weather variability (Gudimov et al., 2011). In this study, our thesis is that the recent advances in stoichiometric nutrient recycling theory along with the ominous prospect of a shift towards a different climatic regime make compelling the revisit of our contemporary modeling practices. Yet, any future attempts to increase the complexity of our

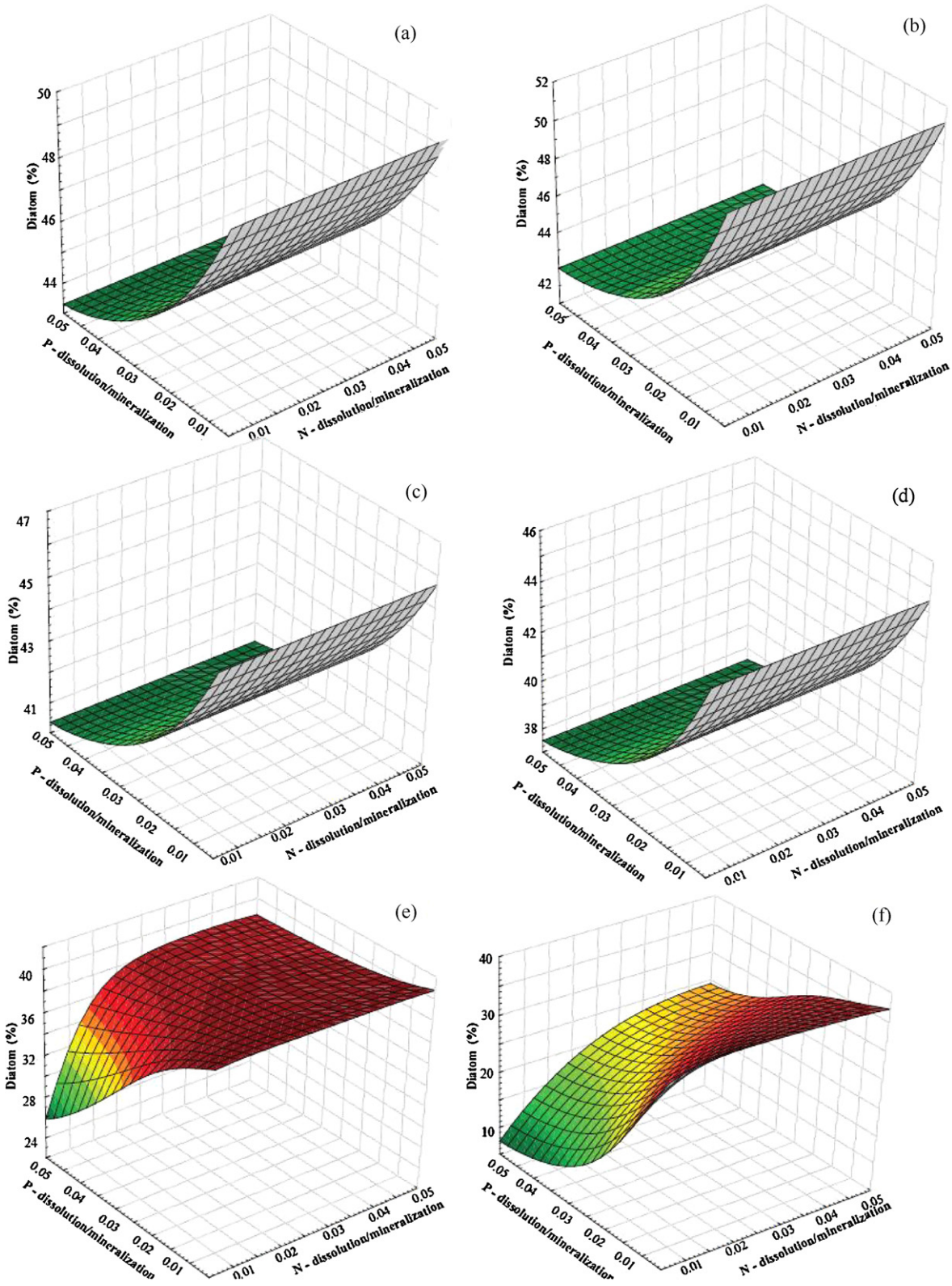

Fig. 4. Diatom percentage contribution to the total phytoplankton biomass against phosphorus and nitrogen dissolution/mineralization rates in (a,b) oligo-, (c,d) meso-, and (e,f) eutrophic environments. Left panels represent the present water temperature conditions, while the right panels correspond to warming scenario of approximately +2 °C.

models require sober evaluation of the inference drawn from the current generation of mathematical models and impartial identification of the knowledge gaps about the role of the nutrient mechanisms on ecosystem functioning.

4.1. Lake trophic status and nutrient recycling rates

Of the parameters reproducing phosphorus recycling into the system, our modeling study highlights the fraction of diatom basal

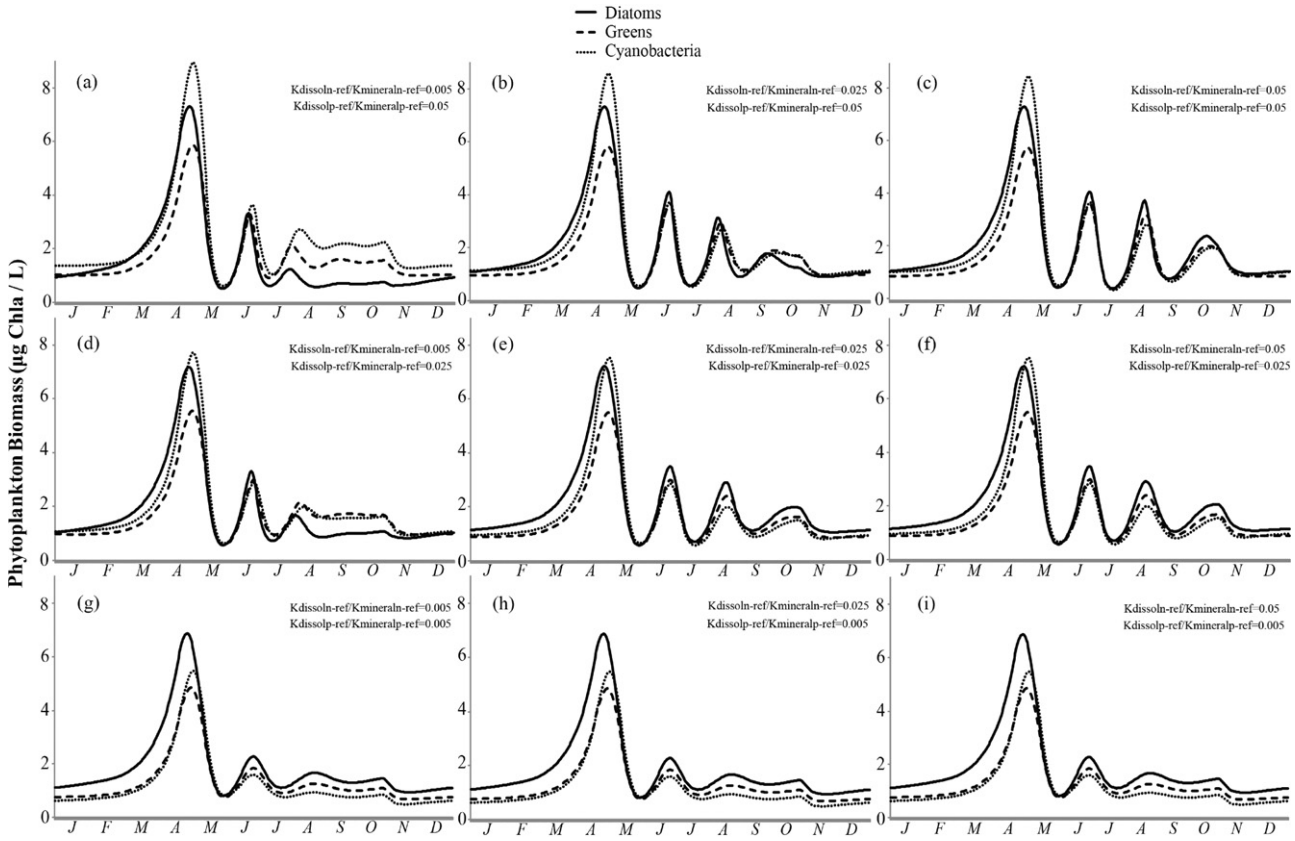

Fig. 5. Seasonal cycles of diatoms, cyanobacteria, and green algae in a eutrophic environment with nine (9) combinations of nitrogen and phosphorus dissolution/mineralization rates. These experiments are based on temperature forcing that represents the present condition.

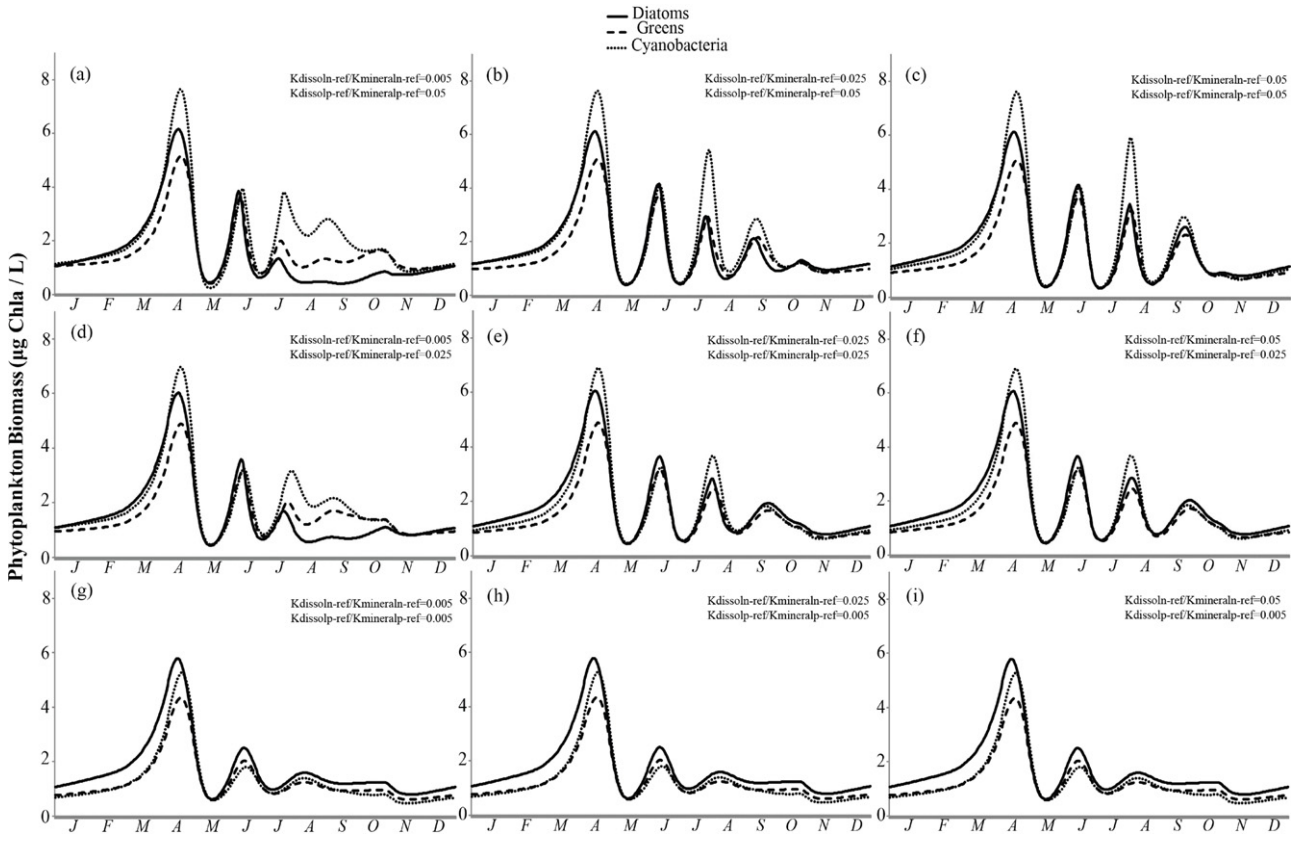

Fig. 6. Seasonal cycles of diatoms, cyanobacteria, and green algae in a eutrophic environment and nine (9) combinations of nitrogen and phosphorus mineralization/dissolution rates. These experiments are based on temperature forcing that represents a warming scenario of approximately +2 °C.

metabolism excreted as phosphate to be an important governing factor of phytoplankton abundance when oligotrophic and mesotrophic conditions are experienced. This result is not surprising, as earlier work from De Pinto et al. (1986) similarly asserted that the non-predatory algal death and the subsequent lysis with the immediate release of stored excess inorganic phosphorus is a significant recycling process, capable of inducing oscillatory patterns even in lakes that receive high external phosphorous loadings. Importantly, the same study also showed that the intracellular phosphorus content of the dying phytoplankton cells can influence the amount recycled, as phosphorus cell levels greater than the minimum cell quota appear to release higher P amounts for a given decay rate (De Pinto et al., 1986). The second step of the conversion of algal biomass phosphorus to bioavailable phosphorus typically involves the microbially-mediated stoichiometric regeneration of the more tightly bound organic cell phosphorus. In our analysis, the bacterial mineralization appears to be less influential relative to the direct phosphate release in oligotrophic settings, but does exert more significant control on phytoplankton variability with the eutrophic scenario; a result that is on par with Kamarainen et al.'s (2009) recent findings in the eutrophic Lake Mendota. While inherently difficult to experimentally/empirically delineate the relative impact of the two processes, our modeling analysis suggests that both can influence the magnitude and duration of the spring bloom as well as the emergence of secondary oscillations in the stratified period (Fig. S10). However, we also note the latter pathway is deterministically conceptualized by a two-step mechanism, $POP \overset{dissolution}{\longrightarrow} DOP \overset{mineralization}{\longrightarrow} PO_4$, and thus its efficiency is conditional upon both the dissolution and mineralization activity of the microbial decomposer community.

One controversial assumption typically incorporated in the current generation of aquatic biogeochemical models is the postulation that nutrient regeneration is proportional to biomass and thus the proportion of net production regenerated (or the regeneration efficiency) is approximately similar among different trophic states. This assumption appears to contradict empirical evidence that nutrient regeneration efficiencies (e.g., high relative prokaryotic heterotrophic biomass, higher bacterial growth efficiency, elevated microbial respiration rates) may be higher in oligotrophic than in eutrophic systems (Cotner and Biddanda, 2002). However, Hudson et al. (1999) challenged this paradigm of greater regeneration efficiency in low productivity systems. In particular, the phosphorus recycling patterns in twenty lakes, spanning a fairly wide trophic gradient (1–80 $\mu g\ TP\ L^{-1}$), indicated that about 20% per day of the particulate phosphorus pool was subjected to mineralization; that is, an amount of phosphorus equal to the particulate phosphorus pool was released into both nutrient-poor and nutrient-rich systems by regeneration mechanisms every five days. In the context of operational modeling, the uncertainty in regards to the relative role of the microbial loop across different trophic states can be a missing pivotal element when projecting future ecosystem responses under alternative loading/climatic regimes. For example, the assignment of high values to the fraction of plankton metabolism that is directly returned into the system as dissolved phase inorganic phosphorus is an effective strategy to simultaneously match the typically high summer chlorophyll *a* levels and low phosphate concentrations in eutrophic environments (Gudimov et al., 2010; Ramin et al., 2011). Yet, the same model parameterization can conceivably disengage the summer phytoplankton growth from the exogenous nutrient loading, as it postulates increased phytoplankton reliance upon regenerated nutrient fluxes. Coupled with the assumption of constant nutrient regeneration efficiency though, this calibration practice tends to moderate the projected system response to loading reduction scenarios (Gudimov et al., 2011). Because the latter point casts doubt on the credibility of many of the contemporary eutrophication model predictions, we caution that any calibration exercise should prudently consider the relative contribution of other potentially important nutrient sources (i.e., internal loading, episodic events) that may intermittently fuel epilimnetic algal growth, and therefore minimize the likelihood of misstating the role of microbial loop as a nutrient supplier, especially in the summer epilimnion (Kamarainen et al., 2009; Gudimov et al., 2011).

4.2. Lake thermal dynamics and nutrient regeneration mechanisms

Counter to the findings of our recent work with other facets of the plankton characterization (Zhao et al., 2008a,b), the present results were significantly driven by the variability of the lake thermal structure. The signature of the water temperature on plankton dynamics can explain the nearly consistent extraction of two principal components (seasonal modes) mainly associated with the cold and warm periods of the year. In contrast, Zhao et al. (2008a,b) frequently reported three distinct seasonal modes, depicting the variability of the spring bloom, the summer stratification, and the period of complete mixing. The parameters associated with planktonic recycling processes cannot evidently exert significant control on aspects of the lake phenology, such as the timing and duration of the spring bloom, as growth/grazing strategies and nutrient kinetics do (Zhao et al., 2008a,b). The nature of the causal link between temperature and plankton biomass was plausibly positive during the seasonal modes associated with the cooler months of the year. By contrast, the negative relationship between temperature and zooplankton biomass may partly reflect the predominance of the temperature-dependent basal metabolic losses over the animal growth during the rest of the year, especially when the consumers are faced with inadequate food abundance and quality. This trend subsequently deprives the epilimnetic environment with the nutrient subsidies from the zooplankton recycling mechanisms, thereby inducing negative feedback to the standing phytoplankton biomass. The only deviation from this general pattern was the zooplankton variability during the stratified period in the eutrophic environment, which was split into two distinct modes reflecting the manifestation of (approximately) two-month period phytoplankton–zooplankton oscillations in response to the increased nutrient loading (Fig. S6); the so-called Rosenzweig's enrichment paradox (Roy and Chattopadhyay, 2007). In addition, our analysis provides evidence that the warming conditions may magnify the amplitude and frequency of the prey–predator oscillations, and thus act as a destructive force on system stability. This finding is in complete alignment with other predictions that draw parallels between the effects of global warming and nutrient enrichment on plankton dynamics (Kilham et al., 1996; Porter et al., 1996). Although Rosenzweig's concept has been severely criticized in the literature as being a mere theoretical artifact (Abrams and Walters, 1996), we believe that it highlights the possibility of a climate-induced reconfiguration of trophic relationships and/or an increased uncertainty on the dynamics of consumer–food systems (Scheffer, 1998; Mooij et al., 2005; Shimoda et al., 2011).

Despite the inherently difficult task to delineate the effects of climate change on lake phenology, the profound changes induced from different nutrient loading regimes may be modulated by climate warming (Shimoda et al., 2011). The climate-induced intensification of lake stratification can presumably magnify the severity of nutrient limitation, thereby promoting changes in the composition of summer algal assemblages in oligo- and mesotrophic epilimnetic environments (Anneville et al., 2005; Law et al., 2009). Empirical evidence suggests that such resource-limited environments typically favour CS strategists, comprising stress-tolerant

species with functional properties (e.g., mixotrophy, motility) that allow them to survive at low nutrient levels and grow faster than S species (Elliott et al., 2000; Reynolds, 2006). In this context, our modeling analysis suggests that increased recycling rates can potentially counterbalance changes in the severity of the phosphorous limitation status and may alleviate the repercussions of warmer conditions in oligo- and mesotrophic environments (i.e., similar patterns between Fig. 2a,c and b,d). On the other hand, systems closer to the dichotomy boundary between N and P limitation may experience distinct changes in regards to the composition of their algal assemblages, as differential N recycling relative to P may trigger shifts in favour of certain functional groups (e.g., our eutrophic scenario). This prediction could also have implications on the recent hypothesis that the climate change may be a potential catalyst for more frequent cyanobacteria blooms in the summer (Legnani et al., 2005; Paerl and Huisman, 2008; Johnk et al., 2008). Their higher optimal temperature for growth along with the increased stability of the water column (i.e., reduced vertical turbulent mixing) are likely to offer competitive advantages to cyanobacteria when lakes experience elevated temperatures (e.g., Dokulil and Teubner, 2000; Johnk et al., 2008). In this context, it is reasonable to assume that the nature of the nutrient recycling rates may also influence the delicate competition balance among the typical residents of the epilimnetic phytoplankton assemblages, thereby leading to cyanobacteria dominance even in settings that would not normally favour such structural shifts. Finally, we note that empirical evidence in support of the likelihood that the differential nutrient recycling can induce changes at the level of phytoplankton community composition does exist, but it has been associated with the stoichiometrically-driven zooplankton release and not with the microbially-mediated nutrient regeneration per se (MacKay and Elser, 1998; Elser and Urabe, 1999).

If we assume that the prolonged lake stratification may indeed increase the dependence on nutrient regeneration mechanisms, then another interesting research question arising is how an epilimnetic environment subject to rapid nutrient turnover rates and to periodic partial mixing due to episodic precipitation events can shape the interspecific plankton competition patterns and ultimately the food web configuration (Capblancq, 1990; Jorgensen and Padisak, 1996; Becker et al., 2008). Current limnological theory predicts that saturating pulses of limiting nutrients likely favour algal species with the capacity to sustain elevated maximum uptake rates and store the largest amount of nutrients relative to their minimum requirements (Suttle et al., 1987). However, it is also recognized that different systems can exhibit distinctly different response that is primarily determined by the internal structure of the food webs (Cottingham and Schindler, 2000). In the same context, Stone and Berman (1993) contended that small-scale nutrient pulses are not necessarily a spark for indiscriminate positive feedback growth that ultimately leads to system destabilization. Rather, major food web reconfiguration and an ecosystem productivity increase as a whole can be achieved from nutrient pulses of a particular range of input frequencies and under a particular set of conditions. Notably, a unique aspect of Stone and Berman's (1993) work was the explicit consideration of time delays among the various ecological processes modeled. For the sake of simplicity, this feature is missing from our (and other) models, but it must be noted that certain aspects of nutrient recycling are hardly instantaneous processes and this simplification may conceal ecologically meaningful insights.

4.3. Plankton stoichiometry and nutrient recycling

Recent empirical evidence suggests that the assumption of strict element homeostasis cannot adequately explain *Daphnia* dynamics in P-deficient environments (Ferrão-Filho et al., 2007), and our analysis highlights the optimal stoichiometric P:C of the P-rich herbivores, $P/C_{opt}(CL)$, along with fraction of phosphate egested during their feeding, $FE_{PO4}(CL)$, as important drivers of the plankton dynamics. The positive relationship between the former parameter and phytoplankton biomass is partly related to the typically made assumption that zooplankton excretion of phosphorus is proportional to its somatic content. Specifically, our model postulates a two-step mechanism through which zooplankton homeostasis is maintained: (i) animals remove nutrient elements in closer proportion to their somatic ratios than to the seston elemental ratio during the digestion and assimilation process (Arhonditsis and Brett, 2005b; Zhao et al., 2008b); and (ii) once the somatic requirements are met, the stoichiometric signature of the excreted material is strictly determined by the consumer elemental composition. Based on this conceptualization, the P-rich animals (e.g., *Daphnia*) should contribute a significant proportion of the excess carbon and nitrogen during their feeding (high C:P and N:P), but subsequently have higher release rates of phosphorus per unit of biomass due to excretion of their metabolic by-products or decomposition of dead material, e.g., tissues, carapaces (low C:P and N:P). In this regard, our modeling analysis is on par with the predictions of the stoichiometric theory, in that P-rich animals can modulate the nature of the sedimentation fluxes, but the two counterbalancing processes moderate the compositional changes of the settling particulate material across different trophic states. In particular, the shift from the eutrophic to the oligotrophic state does increase both the C:P (from 56 to 61 mg C/mg P) and N:P (from 5.9 to 8.2 mg N/mg P) ratios of the particulate fluxes, but this increase may not be as pronounced as typically presented in the literature (Elser and Urabe, 1999; Vanni, 2002).

The alternative hypothesis proposed to explain the homeostatic regulation is that animals maintain their somatic ratio through post-absorptive mechanisms and therefore P-deficient diets can lead to dramatic reduction of the consumer P excretion/respiration rates and maximization of the P assimilation efficiency (Elser and Urabe, 1999). According to the latter hypothesis, we can use the analogy of a cup being filled to describe the capacity of individuals to manage resource accumulation: at first, there is negligible turnover, followed by overflow (i.e., turnover) as the optimal quota is met (Jobling, 2004). In this case, although some animals can excrete in organic forms (e.g., urea), most nutrients are recycled in inorganic forms (e.g., ammonia, phosphate) and thus the excretion rates are tightly related to the ambient nutrient levels (Vanni, 2002). While experimental work in laboratory settings appears to render support to the latter hypothesis (Urabe et al., 2002; Darchambeau et al., 2003), the robustness of its predictions at an ecosystem scale remains largely unexplored (Vanni et al., 2002). Further, Arhonditsis and Brett (2005b) noted that a model parameterization that assigns a higher portion of the recycled material into the dissolved-phase pool resulted in unrealistically high concentrations of the non-limiting elements (ammonium) in the water column relative to the observed levels in Lake Washington. On the other hand, a follow-up analysis that explicitly considers the dynamic handling of substrates within a zooplankter negates (or mitigates) the extreme effects of resource enrichment, as manifested in classical prey–predator models, and reproduces reasonably well "real-world" dynamics (Perhar et al., submitted manuscript). Because the relative importance of the pre- versus post-absorption mechanisms of food processing and their ramifications for ecosystem functioning have not been unequivocally addressed in the contemporary literature (DeMott et al., 1998; Elser and Foster, 1998; Arhonditsis and Brett, 2005b; Zhao et al., 2008b), we stress that the representation of the stoichiometric variability of consumer-driven nutrient recycling is one of the aspects of the current generation of plankton models that needs to be revisited.

In conclusion, our modeling analysis reinforced the (oftentimes neglected) notion that nutrient recycling mechanisms can significantly influence the predictions of any aquatic biogeochemical modeling exercise. The recycled material and the associated energy fluxes can be significant drivers in low as well as in high-productivity ecosystems depending on the period of the year examined. This result is partly driven by the underlying assumption that nutrient regeneration is proportional to biomass and thus the fraction of net production regenerated (or the regeneration efficiency) is approximately similar among different trophic states. Because the latter point remains to be resolved as of yet, we caution that the contemporary calibration practices should carefully consider the relative contribution of other potentially important nutrient sources (i.e., internal loading, episodic events) that may intermittently fuel epilimnetic algal growth. Non-predatory algal death and the subsequent lysis with the immediate release of stored excess inorganic phosphorus is a significant recycling process, capable of inducing oscillatory patterns even in lakes that receive high external phosphorous loadings. Warmer climatic conditions and longer stratification periods will increase the dependence of lakes on nutrient regeneration rates, but the trophic status of a given system along with the associated abiotic conditions and the structure of the biotic communities may be equally important. The lake productivity response, however, is non-linear and non-monotonic and is modulated by the type of nutrient limitation (nitrogen or phosphorus) experienced. In addition, our analysis suggests that the warming conditions may magnify the amplitude and frequency of the prey–predator oscillations, which in turn highlights the possibility of a climate-induced reconfiguration of trophic relationships and/or an increased uncertainty on the dynamics of consumer–food systems. The proper representation of the stoichiometric variability of consumer-driven nutrient recycling is one of the key aspects of aquatic biogeochemical models that should be refined.

Acknowledgments

Funding for this study was provided by the National Sciences and Engineering Research Council of Canada (NSERC, Discovery Grants), Ministry of Research and Innovation (Early Researcher Award granted to George Arhonditsis). Maryam Ramin and Gurbir Perhar have received support from the Natural Sciences and Engineering Research Council of Canada (Doctoral Scholarships). Yuko Shimoda has received support from William G. Dean Queen Elizabeth II Graduate Scholarship in Science & Technology (School of Graduate Studies, University of Toronto).

Appendix A. Supplementary data

Supplementary data associated with this article can be found, in the online version, at http://dx.doi.org/10.1016/j.ecolmodel.2012.04.018.

References

Abrams, P.A., Walters, C.J., 1996. Invulnerable prey and the paradox of enrichment. Ecology 77, 1125–1133.
Anneville, O., Gammeter, S., Straile, D., 2005. Phosphorus decrease and climate variability: mediators of synchrony in phytoplankton changes among European peri-alpine lakes. Freshwater Biology 50, 1731–1746.
Arhonditsis, G.B., Winder, M., Brett, M.T., Schindler, D.E., 2004a. Patterns and mechanisms of phytoplankton variability in Lake Washington (USA). Water Research 38, 4013–4027.
Arhonditsis, G.B., Brett, M.T., DeGasperi, C.L., Schindler, D.E., 2004b. Effects of climatic variability on the thermal properties of Lake Washington. Limnology and Oceanography 49, 256–270.
Arhonditsis, G.B., Brett, M.T., 2005a. Eutrophication model for Lake Washington (USA) Part I. Model description and sensitivity analysis. Ecological Modelling 187, 140–178.
Arhonditsis, G.B., Brett, M.T., 2005b. Eutrophication model for Lake Washington (USA) Part II. Model calibration and system dynamics analysis. Ecological Modelling 187, 179–200.
Arhonditsis, G.B., Qian, S.S., Stow, C.A., Lamon, E.C., Reckhow, K.H., 2007. Eutrophication risk assessment using Bayesian calibration of process-based models. Application to a mesotrophic lake. Ecological Modelling 208, 215–229.
Azam, F., Fenchel, T., Field, J.G., Gray, J.S., Meyer-Rei1, L.A., Thingstad, F., 1983. The ecological role of water-column microbes in the sea. Marine Ecology Progress Series 10, 257–263.
Azam, F., Malfatti, F., 2007. Microbial structuring of marine ecosystems. Nature Reviews Microbiology 5, 782–791.
Becker, V., Huszar, V.L.M., Naselli-Flores, L., Padisak, J., 2008. Phytoplankton equilibrium phases during thermal stratification in a deep subtropical reservoir. Freshwater Biology 53, 952–963.
Berman, T., Bechemin, C., Maestrini, S.Y., 1999. Release of ammonium and urea from dissolved organic nitrogen in aquatic ecosystems. Aquatic Microbial Ecology 16, 295–302.
Blenckner, T., Pettersson, K., Padisak, J., 2002. Lake plankton as tracer to discover climate signals. Internationale Vereinigung fuer Theoretische und Angewandte Limnologie Verhandlungen 28, 1324–1327.
Bloem, J., Albert, C., Bar-Gillissen, M.B., Berman, T., Cappenberg, T.E., 1989. Nutrient cycling through phytoplankton, bacteria and protozoa, in selectively filtered Lake Vechten water. Journal of Plankton Research 11 (1), 119–131.
Brett, M.T., Arhonditsis, G.B., Mueller, S.E., Hartley, D.M., Frodge, J.D., Funke, D.E., 2005. Non-point-source impacts on stream nutrient concentrations along a forest to urban gradient. Journal of Environmental Management 35, 330–342.
Capblancq, J., 1990. Nutrient dynamics and pelagic food web interactions in oligotrophic and eutrophic environments – an overview. Hydrobiologia 207, 1–14.
Cerco, C.F., Cole, T.M., 1994. CE-QUAL-ICM: a Three-dimensional Eutrophication Model, Version 1.0. User's Guide. US Army Corps of Engineers Waterways Experiments Station, Vicksburg, MS.
Chapin, F.S., Zavaleta, E.S., Eviner, V.T., Naylor, R.L., Vitousek, P.M., Reynolds, H.L., Hooper, D.U., et al., 2000. Consequence of changing biodiversity. Nature 405, 232–242.
Coats, R., Perez-Losada, J., Schladow, G., Richards, R., Goldman, C., 2006. The warming of Lake Tahoe. Climatic Change 76, 121–148.
Costanza, R., d'Arge, R., de Groot, R., Farber, S., Grasso, M., Hannon, B., Limburg, K., et al., 1997. The value of the world's ecosystem services and natural capital. Nature 387 (6230), 255.
Cotner, J.B., Biddanda, B.A., 2002. Small players, large role: microbial influence on biogeochemical processes in pelagic aquatic ecosystems. Ecosystems 5, 105–121.
Cottingham, K.L., Schindler, D.E., 2000. Effects of grazer community structure on phytoplankton response to nutrient pulses. Ecology 81, 183–200.
Darchambeau, F., Færøvig, P.J., Hessen, D.O., 2003. How Daphnia copes with excess carbon in its food. Oecologia 136, 336–346.
Davidson, K., 1996. Modelling microbial food webs. Marine Ecology Progress Series 145, 279–296.
DeAngelis, D.L., 1992. Dynamics of Nutrient Cycling and Food Webs. Chapman & Hall, London.
De Pinto, J.V., Young, T.C., Bonner, J.S., Wodgers, P.W., 1986. Microbial recycling of phytoplankton phosphorus. Canadian Journal of Fisheries and Aquatic Sciences 43, 336–342.
DeMott, W.R., Gulati, R.D., Siewertsen, K., 1998. Effects of phosphorus-deficient diets on the carbon and phosphorus balance of Daphnia magna. Limnology and Oceanography 43 (6), 1147–1161.
Devine, J.A., Vanni, M.J., 2002. Spatial and seasonal variation in nutrient excretion by benthic invertebrates in a eutrophic reservoir. Freshwater Biology 47 (6), 1107–1121.
Dokulil, M., Teubner, K., 2000. Cyanobacterial dominance in lakes. Hydrobiologia 438, 1–12.
Ejsmont-Karabin, J., Gorelysheva, Z., Kalinowska, K., Węgleńska, T., 2004. Role of zooplankton (Ciliata, Rotifera and Crustacea) in phosphorus removal from cycling: lakes of the river Jorka watershed (Masurian Lakeland, Poland). Polish Journal of Ecology 52, 275–284.
Elliott, J.A., Reynolds, C.S., Irish, T.E., 2000. The diversity and succession of phytoplankton communities in disturbance-free environments, using the model PROTECH. Archiv für Hydrobiologie 149, 241–258.
Elser, J.J., Foster, D.K., 1998. N:P stoichiometry of sedimentation in lakes of the Canadian shield: relationships with seston and zooplankton elemental composition. Ecoscience 5, 56–63.
Elser, J.J., Urabe, J., 1999. The stoichiometry of consumer-driven nutrient recycling, theory, observations, and consequences. Ecology 80, 735–751.
Fasham, M.J.R., Ducklow, H.W., McKelvie, S.M., 1990. A nitrogen based model of plankton dynamics in the oceanic mixed layer. Journal of Marine Research 48, 591–639.
Ferrão-Filho, A.D.S., Tessier, A.J., Demott, W.R., 2007. Sensitivity of herbivorous zooplankton to phosphorus-deficient diets: testing stoichiometric theory and the growth rate hypothesis. Limnology and Oceanography 52, 407–415.
Flynn, K.J., Davidson, K., Cunningham, A., 1996. Prey selection and rejection by a microflagellate; implications for the study and operation of microbial food webs. Journal of Experimental Marine Biology and Ecology 196, 357–372.
Goldman, J.C., 1984. Conceptual role for micro-aggregates in pelagic surface waters. Bulletin of Marine Science 35, 462–476.

Gudimov, A., Stremilov, S., Ramin, M., Arhonditsis, G.B., 2010. Eutrophication risk assessment in Hamilton Harbour: system analysis and evaluation of nutrient loading scenarios. Journal of Great Lakes Research 36, 520–539.
Gudimov, A., Ramin, M., Labencki, T., Wellen, C., Shelar, M., Shimoda, Y., Boyd, D., Arhonditsis, G.B., 2011. Predicting the response of Hamilton Harbour to the nutrient loading reductions, a modeling analysis of the ecological unknowns. Journal of Great Lakes Research 37, 494–506.
Gulati, R.D., Ejsmontkarabin, J., Rooth, J., Siewertsen, K., 1989. A laboratory study of phosphorus and nitrogen-excretion of Euchlanis-Dilatata-Lucksiana. Hydrobiologia 186, 347–354.
Gulati, R.D., Martinez, C.P., Siewertsen, K., 1995. Zooplankton as a compound mineralising and synthesizing system: phosphorus excretion. Hydrobiologia 315, 25–37.
Hamilton, D.P., Schladow, S.G., 1997. Prediction of water quality in lakes and reservoirs Part I. Model description. Ecological Modelling 96, 91–110.
Hudson, J.J., Taylor, W.D., Schindler, D.W., 1999. Planktonic nutrient regeneration and cycling efficiency in temperate lakes. Nature 400, 659–661.
Jassby, A.D., 1999. Uncovering mechanisms of interannual variability from short ecological time series. In: Scow, K.M., Fogg, G.E., Hinton, D.E., Johnson, M.L. (Eds.), Integrated Assessment of Ecosystem Health. CRC Press, Boca Raton, FL, pp. 285–306.
Jobling, M., 2004. On-growing to market size. In: Moksness, E., Kjorsvik, E., Olsen, Y. (Eds.), Culture of Cold-water Marine Fish. Blackwell Science, Oxford, UK, pp. 363–432.
Johnk, K.D., Huisman, J., Sharples, J., Sommeijer, B., Visser, P.M., Stroom, J.M., 2008. Summer heatwaves promote blooms of harmful cyanobacteria. Global Change Biology 14, 495–512.
Jorgensen, S.E., Padisak, J., 1996. Does the intermediate disturbance hypothesis comply with thermodynamics? Hydrobiologia 323, 9–21.
Jorgensen, S.E., Bendoricchio, G., 2001. Fundamentals of Ecological Modelling, third ed. Elsevier, Amsterdam, p. 530.
Kamarainen, A.M., Penczykowski, R.M., Van de Bogert, M.C., Hanson, P.C., Carpenter, S.R., 2009. Phosphorus sources and demand during summer in a eutrophic lake. Aquatic Sciences 71, 214–227.
Kilham, S.S., Theriot, E.C., Fritz, S.C., 1996. Linking planktonic diatoms and climate change using resource theory in the large lakes of the Yellowstone ecosystem. Limnology and Oceanography 41, 1052–1062.
Kowalezewska-Madura, K., Goldyn, R., Szyper, H., 2007. Zooplankton phosphorus excretion in Swarzedzkie Lake (Western Poland) and its influence on phytoplankton. Oceanological and Hydrobiological Studies 36, 3–16.
Law, T., Zhang, W., Zhao, J., Arhonditsis, G.B., 2009. Structural changes in lake functioning induced from nutrient loading and climate variability. Ecological Modelling 220, 979–997.
Legendre, P., Legendre, L., 1998. Numerical Ecology, 2nd edition. Elsevier Science B.V., Amsterdam, The Netherlands, p. 853.
Legnani, E., Copetti, D., Oggioni, A., Tartari, G., Palumbo, M.T., Morabito, G., 2005. Planktothrix rubescens' seasonal dynamics and vertical distribution in Lake Pusiano (North Italy). Journal of Limnology 64, 61–73.
MacKay, N.A., Elser, J.J., 1998. Factors potentially preventing trophic cascades: Food quality, invertebrate predation, and their interaction. Limnology and Oceanography 43, 339–347.
Moloney, C.L., Field, J.G., 1991a. The size-based dynamics of plankton food webs. I. A simulation model of carbon and nitrogen flows. Journal of Plankton Research 13, 1003–1038.
Moloney, C.L., Field, J.G., 1991b. The size-based dynamics of plankton food webs. II. Simulations of three contrasting southern Benguela food webs. Journal of Plankton Research 13, 1039–1092.
Mooij, W.M., Hülsmann, S., De Senerpont Domis, L.N., Nolet, B.A., Bodelier, P.L.E., Boers, P.C.M., et al., 2005. The impact of climate change on lakes in the Netherlands: a review. Aquatic Ecology 39, 381–400.
Mulder, K., Bowden, W.B., 2007. Organismal stoichiometry and the adaptive advantage of variable nutrient use and production efficiency in Daphnia. Ecological Modelling 202, 427–440.
Odum, E.P., 1969. The strategy of ecosystem development. Science 164, 262–270.
Omlin, M., Brun, P., Reichert, P., 2001. Biogeochemical model of Lake Zurich: sensitivity, identifiability and uncertainty analysis. Ecological Modelling 141, 105–123.
Paerl, H.W., Huisman, J., 2008. Climate-Blooms like it hot. Science 320, 57–58.
Peduzzi, P., Herndl, G.T., 1992. Zooplankton activity fueling the microbial loop: differential growth response of bacteria from oligotrophic and eutrophic waters. Limnology and Oceanography 37, 1087–1092.
Peters, R.H., 1983. The Ecological Implication of Body Size. Cambridge University Press, Cambridge.
Pomeroy, L.R., Williams, P.J., Azam, F., 2007. The microbial loop. Oceanography 20, 28–33.
Porter, K.G., Saunders, P.A., Haberyan, K.A., Macubbin, A.E., Jacobsen, T.R., Hodson, R.E., 1996. Annual cycle of autotrophic and heterotrophic production in a small, monomictic Piedmont lake (Lake Oglethorpe): analog for the effects of climatic warming on dimictic lakes. Limnology and Oceanography 41, 1041–1051.
Ramin, M., Stremilov, S., Labencki, T., Gudimov, A., Boyd, D., Arhonditsis, G.B., 2011. Integration of mathematical modeling and Bayesian inference for setting water quality criteria in Hamilton Harbour, Ontario, Canada. Environmental Modelling and Software 26, 337–353.
Reynolds, C.S., 2006. The Ecology of Phytoplankton. Cambridge University Press, Cambridge, pp. 535–539.
Richman, M.B., 1986. Rotation of principal components. International Journal of Climatology 6, 293–335.
Roy, S., Chattopadhyay, J., 2007. Towards a resolution of 'the paradox of the plankton': a brief overview of the proposed mechanisms. Journal of Biosciences 32, 26–33.
Scheffer, M., 1998. Ecology of Shallow Lakes. Chapman and Hall, London.
Sherr, B.F., Sherr, E.B., Berman, T., 1982. Grazing, growth, and ammonium excretion rates of a heterotrophic microflagellate fed with four species of bacteria. Applied and Environmental Microbiology 45, 1196–2120.
Shimoda, Y., Azim, E., Perhar, G., Ramin, M., Kenney, M., Sadraddini, S., Gudimov, A., Arhonditsis, G.B., 2011. Our current understanding of lake ecosystem response to climate change: what have we learnt from the north temperate lakes? Journal of Great Lakes Research 37, 173–193.
Sterner, R.W., Elser, J.J., 2002. Ecological Stoichiometry: The Biology of Elements from Molecules to the Biosphere. Princeton University Press, Princeton, NJ.
Stone, L., Berman, T., 1993. Positive Feedback in aquatic ecosystems: the case of the microbial loop. The Bulletin of Mathematical Biology 55, 919–936.
Suttle, C.A., Stockner, J.G., Harrison, P.J., 1987. Effects of nutrient pulses on community structure and cell size of a freshwater phytoplankton assemblage in culture. Canadian Journal of Fisheries and Aquatic Sciences 44, 1768–1774.
Suttle, C.A., 1994. The significance of viruses to mortality in aquatic microbial communities. Microbial Ecology 28, 237–243.
Taylor, A.H., Joint, I., 1990. Steady-state analysis of the microbial loop in stratified systems. Marine Ecology Progress Series 59, 1–17.
Teubner, K., Crosbie, N.D., Donabaum, K., Kabas, W., Kirschner, A.K.T., Pfister, G., Salbrechter, M., Dokulil, M.T., 2003. Enhanced phosphorus accumulation efficiency by the pelagic community at reduced phosphorus supply: a lake experiment from bacteria to metazoan zooplankton. Limnology and Oceanography 48, 1141–1149.
Urabe, J., Elser, J.J., Kyle, M., Sekino, T., Kawabata, Z., 2002. Herbivorous animals can mitigate unfavourable ratios of energy and material supplies by enhancing nutrient recycling. Ecology Letters 5, 177–185.
Vanni, M.J., 2002. Nutrient cycling by animals in freshwater ecosystems. Annual Review of Ecology and Systematics 33, 341–370.
Vanni, M.J., Flecker, A.S., Hood, J.M., Headworth, J.L., 2002. Stoichiometry of nutrient cycling by vertebrates in a tropical stream: linking species identity and ecosystem processes. Ecology Letters 5, 285–293.
Weisse, T., Müller, H., Pinto-Coelho, R.M., Schweizer, A., Springman, D., Baldringer, G., 1990. Response of the microbial loop to the phytoplankton spring bloom in a large prealpine lake. Limnology and Oceanography 35, 781–794.
Winder, M., Hunter, D.A., 2008. Temporal organization of phytoplankton communities linked to physical forcing. Oecologia 156, 179–192.
Zhao, J.Y., Ramin, M., Cheng, V., Arhonditsis, G.B., 2008a. Plankton community patterns across a trophic gradient: the role of zooplankton functional groups. Ecological Modelling 213, 417–436.
Zhao, J.Y., Ramin, M., Cheng, V., Arhonditsis, G.B., 2008b. Competition patterns among phytoplankton functional groups: how useful are the complex mathematical models? Acta Oecologica 33, 324–344.

EXAMINATION OF THE EFFECTS OF NUTRIENT REGENERATION MECHANISMS ON PLANKTON DYNAMICS USING AQUATIC BIOGEOCHEMICAL MODELING

(Electronic Supplementary Material)

Maryam Ramin, Gurbir Perhar, Yuko Shimoda, George B. Arhonditsis*

Ecological Modeling Laboratory
Department of Physical & Environmental Sciences, University of Toronto,
Toronto, Ontario, Canada, M1C 1A4

* Corresponding author
E-mail: georgea@utsc.utoronto.ca, Tel.: +1 416 208 4858; Fax: +1 416 287 7279

Table S1: Multiple regression models developed for examining the most influential factors (stoichiometric properties, nutrient recycling parameters and abiotic conditions) associated with particulate nitrogen fluxes across the three trophic states

Oligotrophic							
January *(r^2= 0.970)*	$\|\beta\|$	April *(r^2=0 .962)*	$\|\beta\|$	July *(r^2= 0.946)*	$\|\beta\|$	October *(r^2= 0.961)*	$\|\beta\|$
$FBM_{NH4}(D)^*$	0.513	$FBM_{NH4}(D)^*$	0.578	$FE_{NH4}(CL)^*$	0.402	$FBM_{NH4}(D)^*$	0.493
Loading	0.452	$FE_{NH4}(CO)^*$	0.365	$FE_{NH4}(CO)^*$	0.363	$FE_{NH4}(CL)^*$	0.333
$K_{dissoln\text{-}ref}(CY)^*$	0.309	$FBM_{DON}(D)^*$	0.324	$FBM_{NH4}(D)^*$	0.338	$FBM_{PO4}(D)$	0.282
$FBM_{DON}(D)^*$	0.286	$FE_{DON}(CO)^*$	0.205	$FE_{DON}(CL)^*$	0.227	$FBM_{DON}(D)^*$	0.275
$FE_{NH4}(CO)^*$	0.240	$FBM_{NH4}(G)^*$	0.202	$Temperature_{epi}$	0.215	$K_{dissoln\text{-}ref}(CY)^*$	0.251
Mesotrophic							
January *(r^2=0 .949)*	$\|\beta\|$	April *(r^2= 0.949)*	$\|\beta\|$	July *(r^2=0 .944)*	$\|\beta\|$	October *(r^2=0 .959)*	$\|\beta\|$
$FE_{NH4}(CO)^*$	0.548	$FE_{NH4}(CO)^*$	0.498	$FE_{NH4}(CL)^*$	0.427	$FE_{NH4}(CL)^*$	0.453
$FBM_{NH4}(D)^*$	0.405	$FBM_{NH4}(D)^*$	0.478	$FE_{NH4}(CO)^*$	0.367	$FBM_{NH4}(D)^*$	0.427
$FE_{DON}(CO)^*$	0.296	$FE_{DON}(CO)^*$	0.268	$FBM_{NH4}(D)^*$	0.301	$FE_{DON}(CL)^*$	0.258
$Temperature_{epi}$	0.266	$FBM_{DON}(D)^*$	0.265	$Temperature_{epi}$	0.272	$FBM_{NH4}(G)^*$	0.246
$K_{dissoln\text{-}ref}(CY)^*$	0.237	$FBM_{NH4}(G)^*$	0.222	$FE_{DON}(CL)^*$	0.246	$FBM_{DON}(D)^*$	0.239

Eutrophic			
First Mode *(r^2=0 .951)*	$\|\beta\|$	Second Mode *(r^2=0 .900)*	$\|\beta\|$
$FE_{NH4}(CO)$	0.517	$FE_{NH4}(CL)$	0.566
$FBM_{NH4}(D)$	0.324	$FE_{NH4}(CO)^*$	0.428
$FE_{NH4}(CL)$	0.302	$K_{mineralp\text{-}ref}{}^*$	0.369
$FE_{DON}(CO)$	0.284	$FE_{DON}(CL)$	0.327
$FBM_{NH4}(G)$	0.2031	$K_{dissolp\text{-}ref}(CY)^*$	0.302

Symbol $|\beta|$ denotes the absolute value of the standardized regression coefficients.
* Negative sign of the standardized regression coefficients.

Eutrophic environment
First mode: Jan-Jun, Dec; Second mode: Jul-Nov.

Table S2: Multiple regression models developed for examining the most influential factors (stoichiometric properties, nutrient recycling parameters and abiotic conditions) associated with particulate phosphorus fluxes across the three trophic states

Oligotrophic							
January *(r^2=0 .983)*	$\|\beta\|$	April *(r^2=0 .971)*	$\|\beta\|$	July *(r^2= 0.956)*	$\|\beta\|$	October *(r^2= 0.956)*	$\|\beta\|$
Loading	0.805	Loading	0.486	Loading	0.462	Loading	0.577
$FBM_{PO4}(D)^*$	0.318	$FBM_{PO4}(D)^*$	0.475	$Temperature_{epi}$	0.421	$Temperature_{epi}$	0.328
$K_{dissolp\text{-}ref}{}^*$	0.278	$FBM_{DOP}(D)^*$	0.341	$FE_{PO4}(CL)^*$	0.296	$P/C_{OPT}(CL)$	0.321
$Temperature_{epi}$	0.221	$Temperature_{epi}$	0.287	$P/C_{OPT}(CL)$	0.268	$FBM_{PO4}(D)^*$	0.305
$KT_{micref1}$	0.162	$FE_{PO4}(CO)^*$	0.238	$K_{mineralp\text{-}ref}$	0.230	$FE_{PO4}(CL)^*$	0.249
Mesotrophic							
First Mode *(r^2=0 .970)*	$\|\beta\|$	Second Mode *(r^2=0 .945)*	$\|\beta\|$				
$Temperature_{epi}$	0.620	$FE_{PO4}(CO)^*$	0.445				
$FE_{PO4}(CL)^*$	0.345	$FBM_{PO4}(D)^*$	0.408				
$P/C_{OPT}(CL)$	0.311	Loading	0.336				
Loading	0.230	$K_{dissolp\text{-}ref}{}^*$	0.335				
N(CO)	0.203	$FE_{DOP}(CO)^*$	0.282				
Eutrophic							
First Mode *(r^2=0 .961)*	$\|\beta\|$	Second Mode *(r^2=0 .968)*	$\|\beta\|$	Third Mode *(r^2= 0.968)*	$\|\beta\|$		
$Temperature_{epi}$	0.555	$Temperature_{epi}{}^*$	0.730	$FE_{PO4}(CO)^*$	0.622		
$FE_{PO4}(CL)^*$	0.482	$FE_{PO4}(CL)^*$	0.290	$FE_{DOP}(CO)^*$	0.375		
$FE_{DOC}(CL)$	0.286	$FBM_{PO4}(D)^*$	0.253	$Temperature_{epi}$	0.310		
$FE_{DOP}(CL)^*$	0.274	$K_{dissolp\text{-}ref}{}^*$	0.216	$P/C_{OPT}(CO)^*$	0.205		
$FBM_{PO4}(CL)^*$	0.225	Loading	0.194	$FBM_{PO4}(D)^*$	0.198		

Symbol $|\beta|$ denotes the absolute value of the standardized coefficients.

* Negative sign of the standardized coefficients.

Mesotrophic environment

First mode: Jul-Oct; Second mode: Jan-May, Nov-Dec.

Eutrophic environment

First mode: Jun-Oct; Second mode: May, Nov; Third mode: Jan-Apr.

FIGURES LEGENDS

Figure S1: Conceptual diagrams of the modeled plankton food web, carbon, nitrogen, and phosphorus cycles.

Figure S2: Plots of total phytoplankton biomass against the zooplankton stoichiometric properties, zooplankton regulatory coefficient, (N), zooplankton optimum phosphorus to carbon ratio, (P/C_{opt}), zooplankton minimum phosphorus to carbon ratio, (P/C_{min}), and a wide range of total ambient phosphorus concentrations. In these experiments, the critical threshold for mineral phosphorus limitation ($C:P_0$) is set equal to the optimal phosphorus to carbon somatic ratio.

Figure S3: Seasonal variability of nitrogen and phosphorus particulate fluxes in the oligo-, meso- and eutrophic settings. Solid lines correspond to monthly median biomass values, while dashed lines correspond to the 2.5 and 97.5% percentiles of the Monte Carlo runs.

Figure S4: Seasonal variability of diatoms, cyanobacteria, green algae, copepods, cladocerans and carbon particulate fluxes in the oligotrophic environment. Solid lines correspond to monthly median biomass values, while dashed lines correspond to the 2.5 and 97.5% percentiles of the Monte Carlo runs.

Figure S5: Seasonal variability of diatoms, cyanobacteria, green algae, copepods, cladocerans and carbon particulate fluxes in the mesotrophic environment. Solid lines correspond to monthly median biomass values, while dashed lines correspond to the 2.5 and 97.5% percentiles of the Monte Carlo runs.

Figure S6: Seasonal variability of diatoms, cyanobacteria, green algae, copepods, cladocerans and carbon particulate fluxes in the eutrophic environment. Solid lines correspond to monthly median biomass values, while dashed lines correspond to the 2.5 and 97.5% percentiles of the Monte Carlo runs.

Figure S7: Rotated component coefficients for the principal components of phytoplankton biomass across a trophic gradient.

Figure S8: Rotated component coefficients for the principal components of zooplankton biomass across a trophic gradient.

Figure S9: Rotated component coefficients for the principal components of particulate carbon fluxes biomass across a trophic gradient.

Figure S10: Abundance of diatom, cyanobacteria, and green algae in an oligotrophic environment with three (3) different levels of phosphorus mineralization/dissolution rates. Panels (a-c) assume that 10% of the phosphorus excreted from plankton metabolism is phosphate and 65% is in dissolved organic form, while the opposite holds true for panels (d-f). The temperature forcing represents the present conditions.

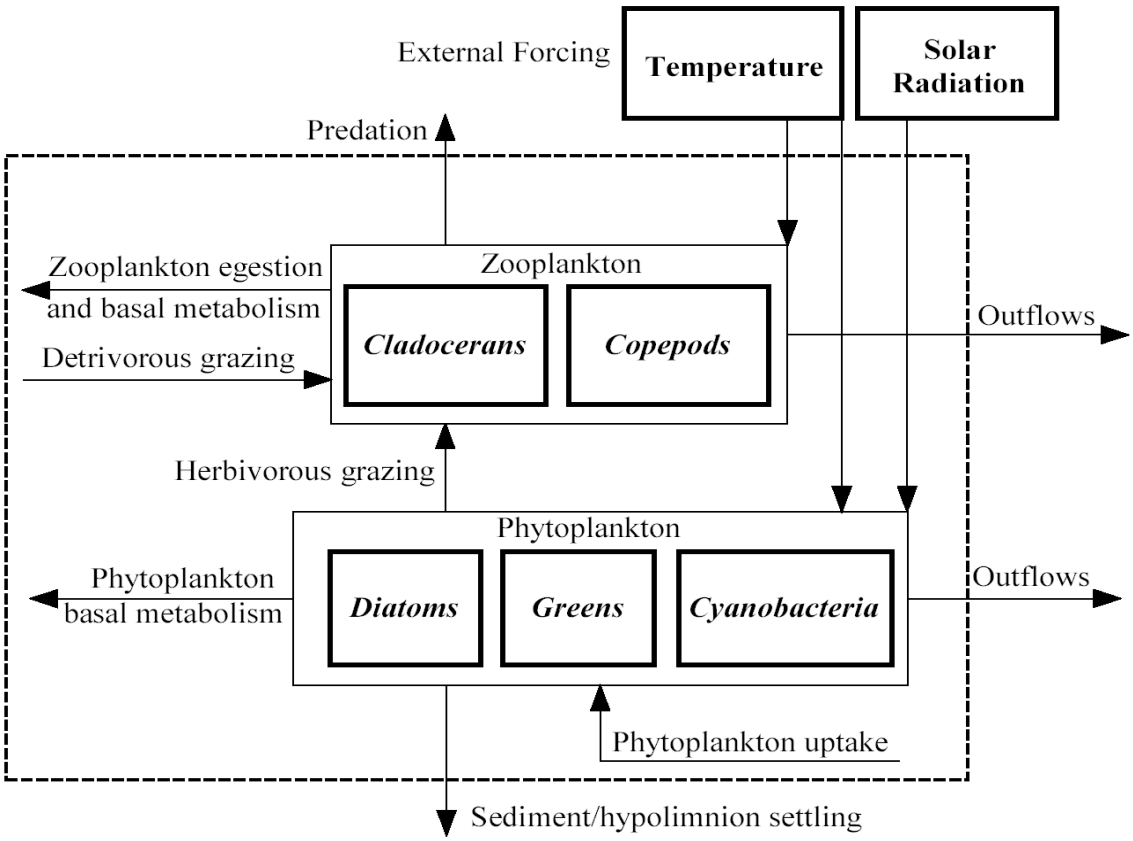
External Forcing
Temperature
Solar Radiation
Predation
Zooplankton egestion and basal metabolism
Detrivorous grazing
Zooplankton
Cladocerans
Copepods
Outflows
Herbivorous grazing
Phytoplankton
Phytoplankton basal metabolism
Diatoms
Greens
Cyanobacteria
Outflows
Phytoplankton uptake
Sediment/hypolimnion settling

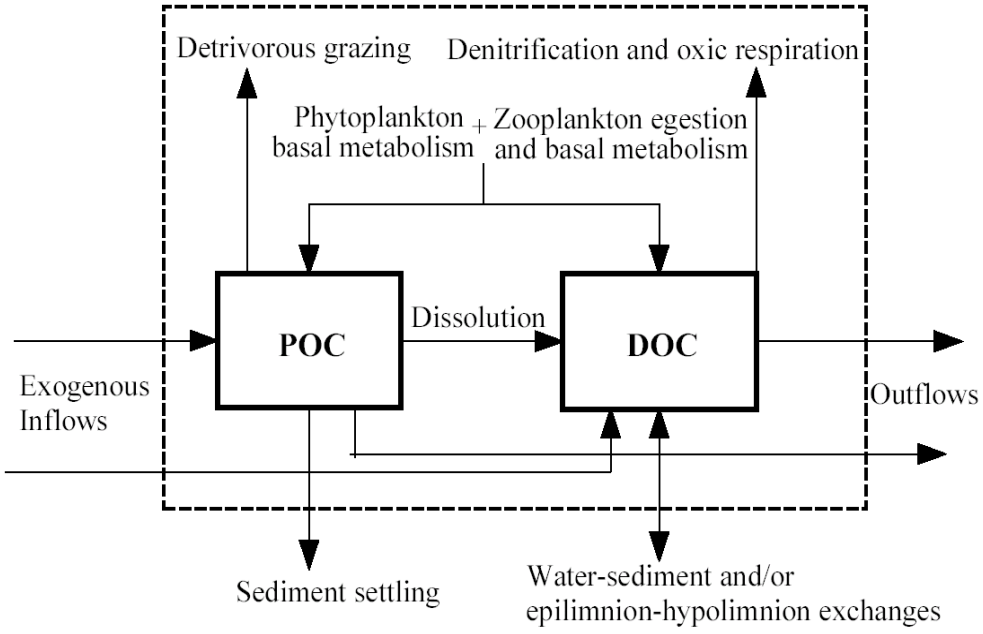
Detrivorous grazing
Denitrification and oxic respiration
Phytoplankton basal metabolism + Zooplankton egestion and basal metabolism
POC
Dissolution
DOC
Exogenous Inflows
Outflows
Sediment settling
Water-sediment and/or epilimnion-hypolimnion exchanges

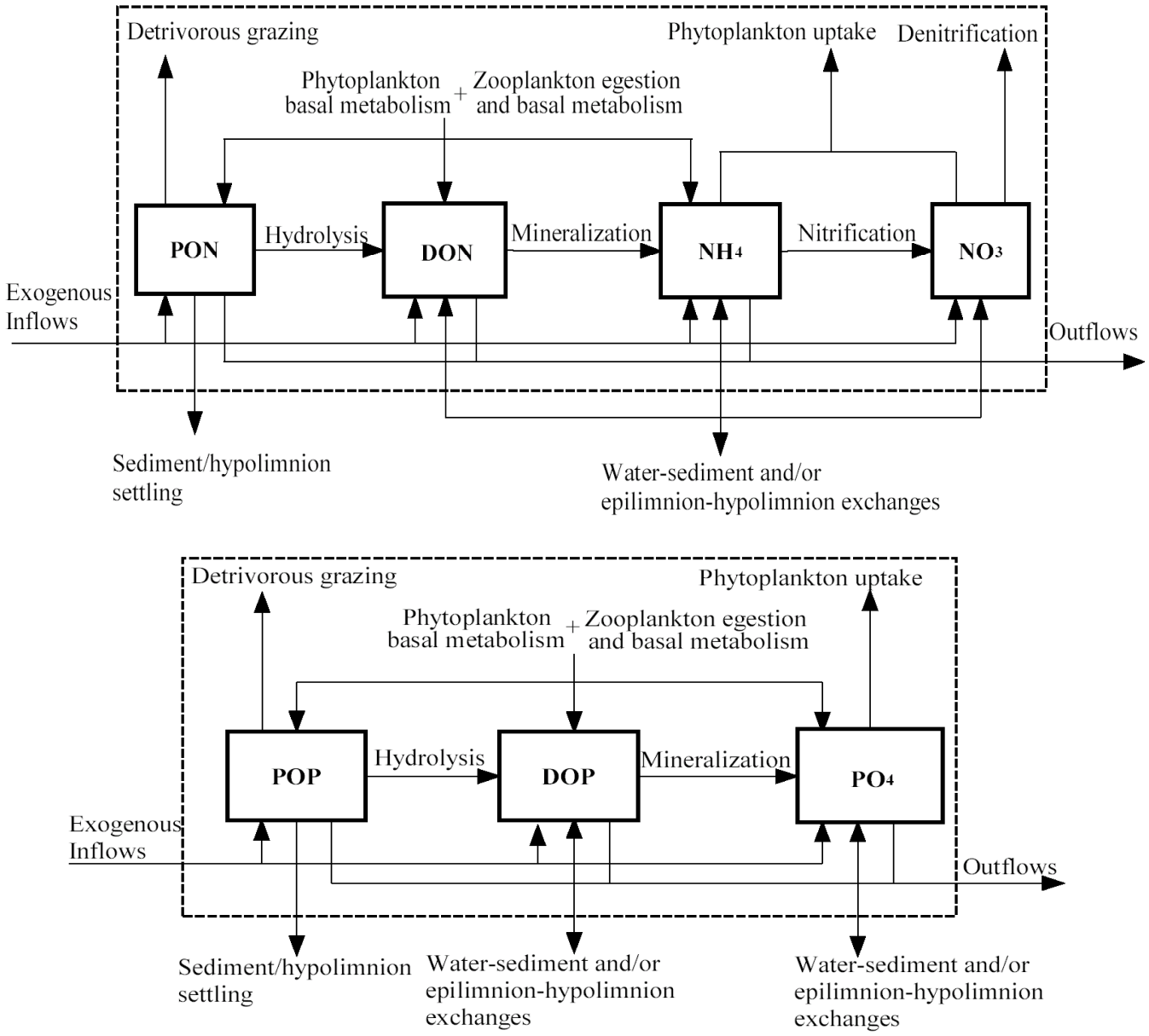
Detrivorous grazing
Phytoplankton uptake
Denitrification
Phytoplankton basal metabolism + Zooplankton egestion and basal metabolism
PON
Hydrolysis
DON
Mineralization
NH4
Nitrification
NO3
Exogenous Inflows
Outflows
Sediment/hypolimnion settling
Water-sediment and/or epilimnion-hypolimnion exchanges
Detrivorous grazing
Phytoplankton uptake
Phytoplankton basal metabolism + Zooplankton egestion and basal metabolism
POP
Hydrolysis
DOP
Mineralization
PO4
Exogenous Inflows
Outflows
Sediment/hypolimnion settling
Water-sediment and/or epilimnion-hypolimnion exchanges
Water-sediment and/or epilimnion-hypolimnion exchanges

Figure S1

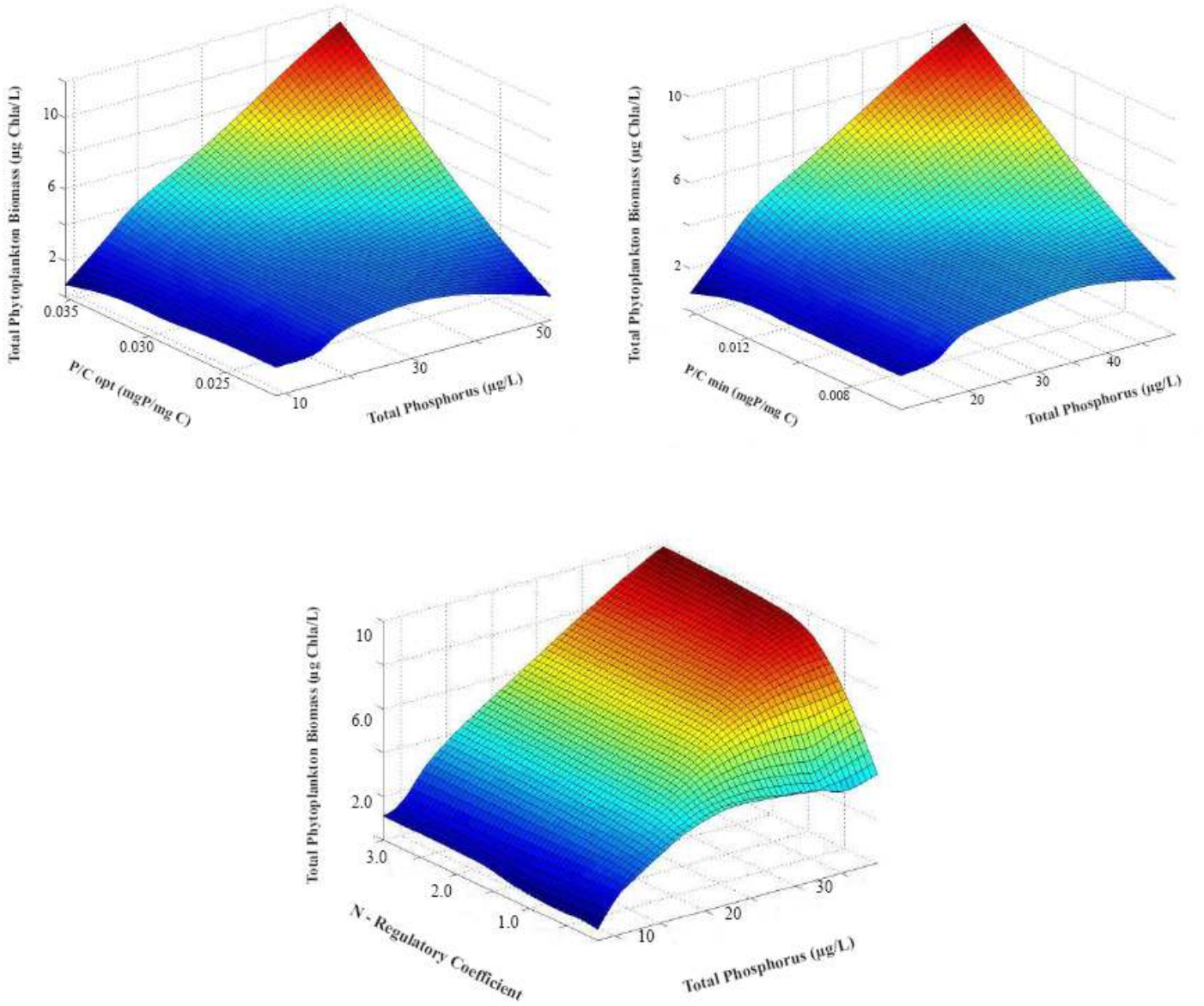
Total Phytoplankton Biomass (µg Chla/L)
10
6
2
0.035
0.030
0.025
P/C opt (mgP/mg C)
10
30
50
Total Phosphorus (µg/L)
Total Phytoplankton Biomass (µg Chla/L)
10
6
2
0.012
0.008
P/C min (mgP/mg C)
20
30
40
Total Phosphorus (µg/L)
Total Phytoplankton Biomass (µg Chla/L)
10
6.0
2.0
3.0
2.0
1.0
N - Regulatory Coefficient
10
20
30
Total Phosphorus (µg/L)

Figure S2

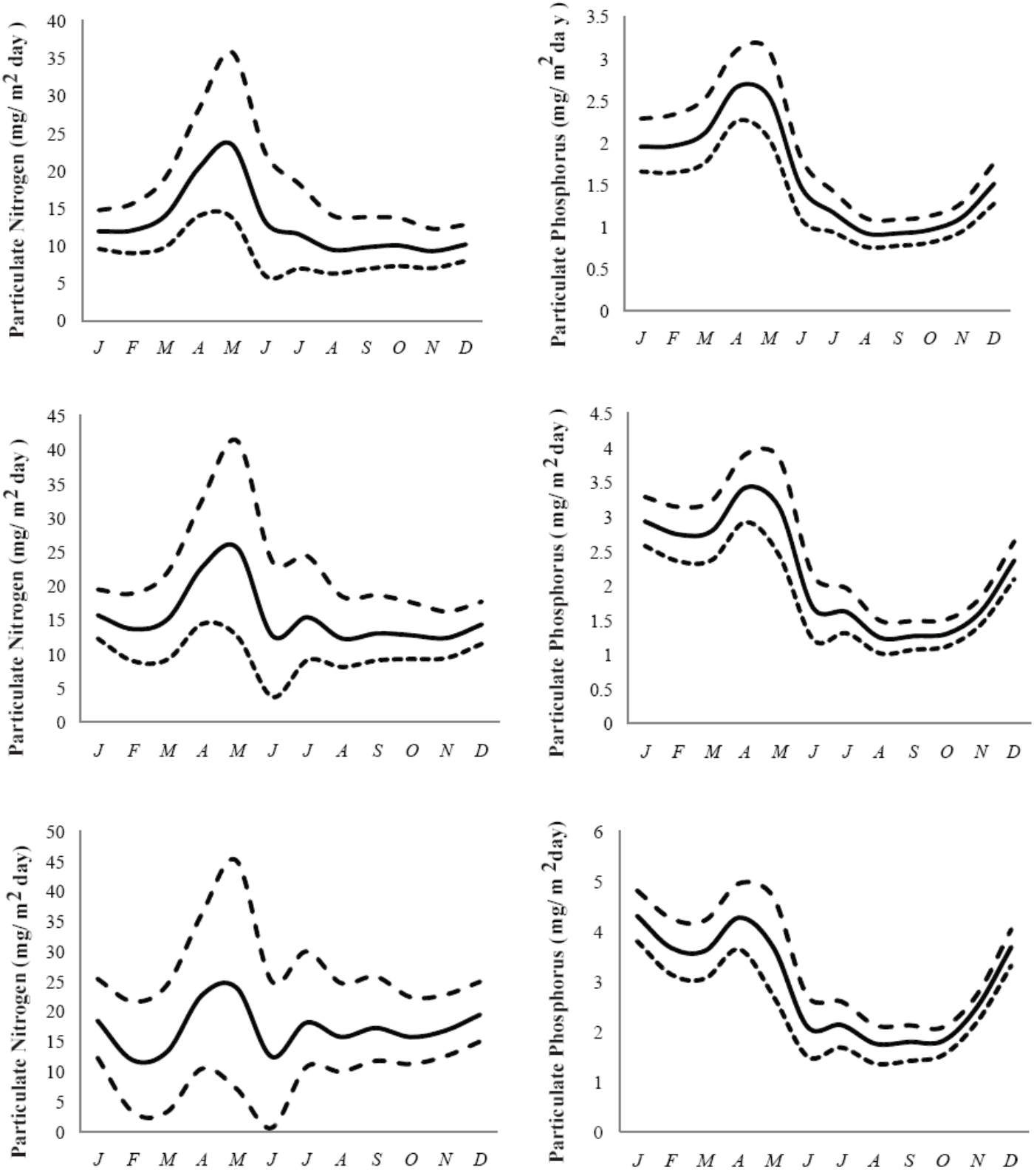
Particulate Nitrogen (mg/ m2 day)
Particulate Phosphorus (mg/ m2 da y)
Particulate Nitrogen (mg/ m2 day)
Particulate Phosphorus (mg/ m 2day)
Particulate Nitrogen (mg/ m2 day)
Particulate Phosphorus (mg/ m 2day)
J F M A M J J A S O N D

Figure S3

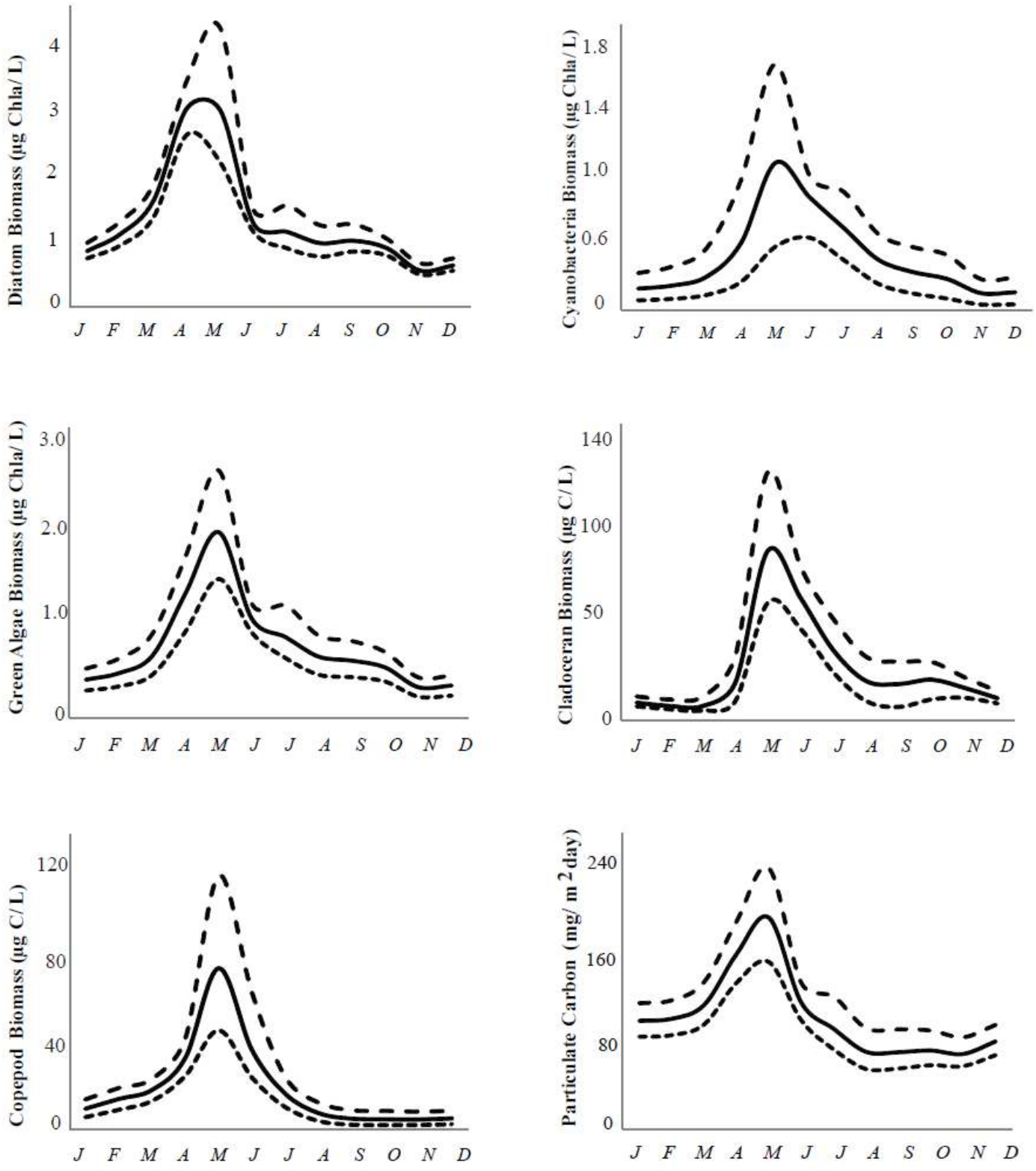
Diatom Biomass (µg Chla/ L)
0
1
2
3
4
J F M A M J J A S O N D
Cyanobacteria Biomass (µg Chla/ L)
0
0.6
1.0
1.4
1.8
J F M A M J J A S O N D
Green Algae Biomass (µg Chla/ L)
0
1.0
2.0
3.0
J F M A M J J A S O N D
Cladoceran Biomass (µg C/ L)
0
50
100
140
J F M A M J J A S O N D
Copepod Biomass (µg C/ L)
0
40
80
120
J F M A M J J A S O N D
Particulate Carbon (mg/ m 2 day)
0
80
160
240
J F M A M J J A S O N D

Figure S4

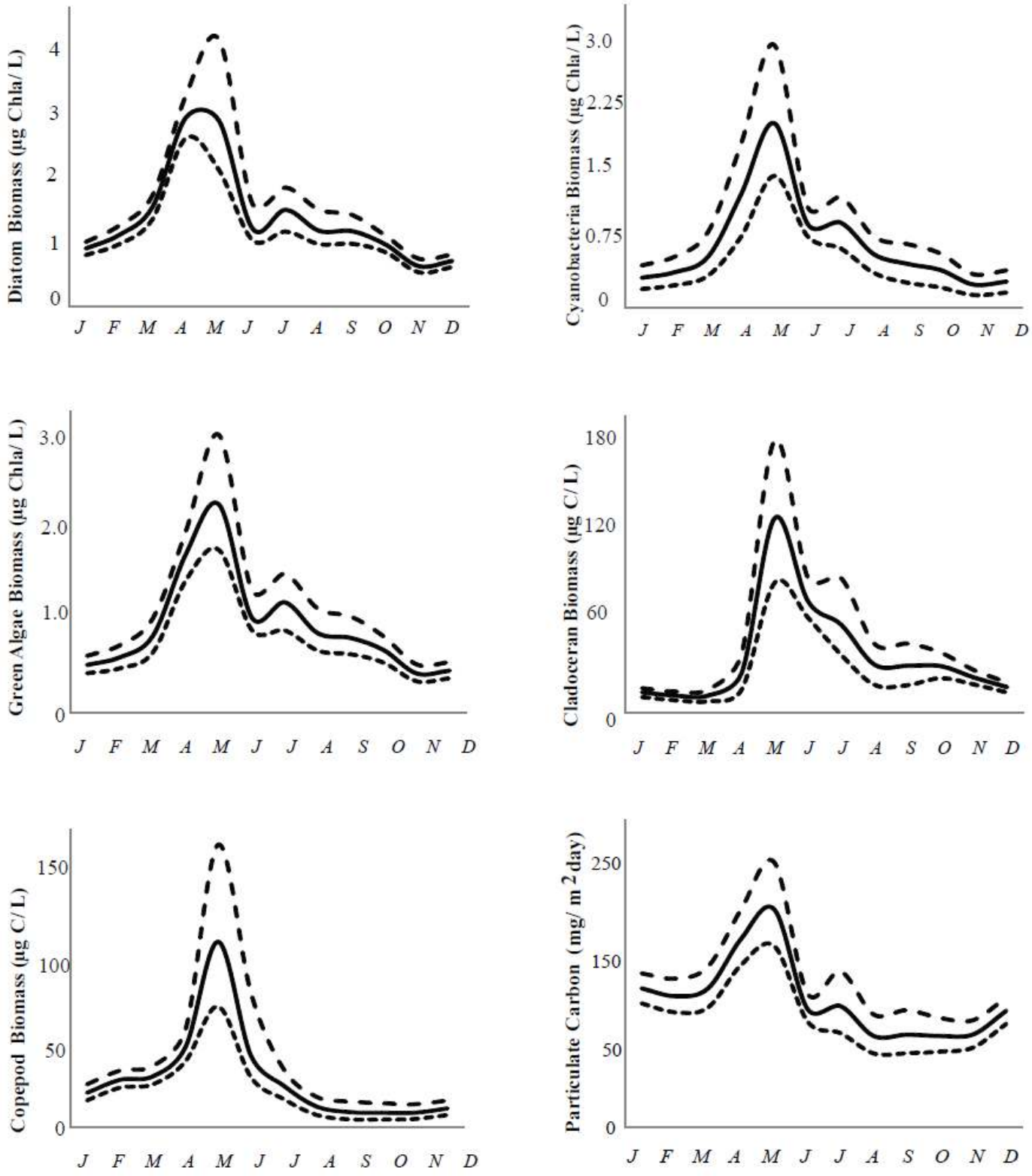
Diatom Biomass (µg Chla/ L)
0
1
2
3
4
J F M A M J J A S O N D
Cyanobacteria Biomass (µg Chla/ L)
0
0.75
1.5
2.25
3.0
J F M A M J J A S O N D
Green Algae Biomass (µg Chla/ L)
0
1.0
2.0
3.0
J F M A M J J A S O N D
Cladoceran Biomass (µg C/ L)
0
60
120
180
J F M A M J J A S O N D
Copepod Biomass (µg C/ L)
0
50
100
150
J F M A M J J A S O N D
Particulate Carbon (mg/ m 2 day)
0
50
150
250
J F M A M J J A S O N D

Figure S5

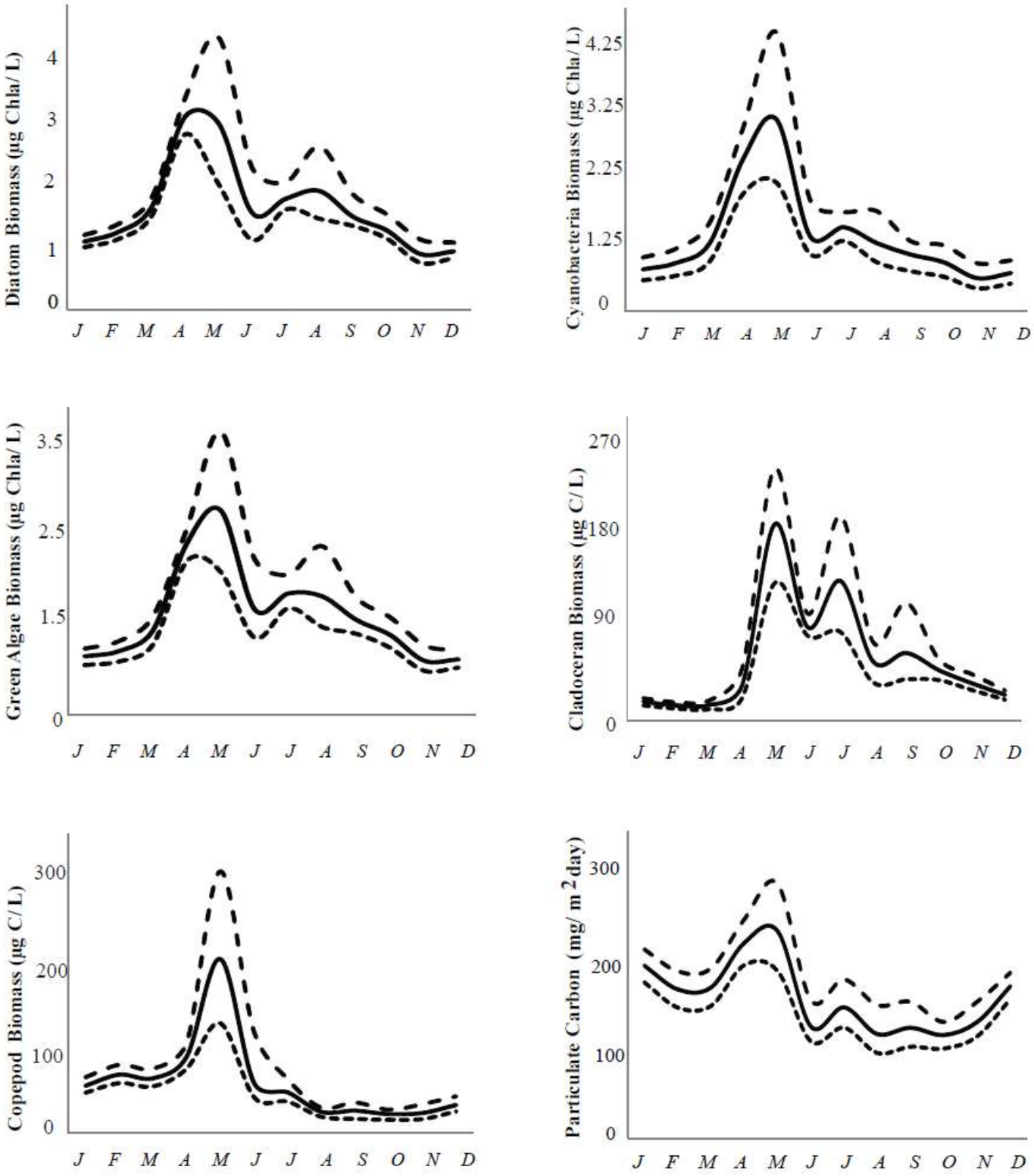
Diatom Biomass (µg Chla/ L)
0
1
2
3
4
J F M A M J J A S O N D
Cyanobacteria Biomass (µg Chla/ L)
0
1.25
2.25
3.25
4.25
J F M A M J J A S O N D
Green Algae Biomass (µg Chla/ L)
0
1.5
2.5
3.5
J F M A M J J A S O N D
Cladoceran Biomass (µg C/ L)
0
90
180
270
J F M A M J J A S O N D
Copepod Biomass (µg C/ L)
0
100
200
300
J F M A M J J A S O N D
Particulate Carbon (mg/ m 2 day)
0
100
200
300
J F M A M J J A S O N D

Figure S6

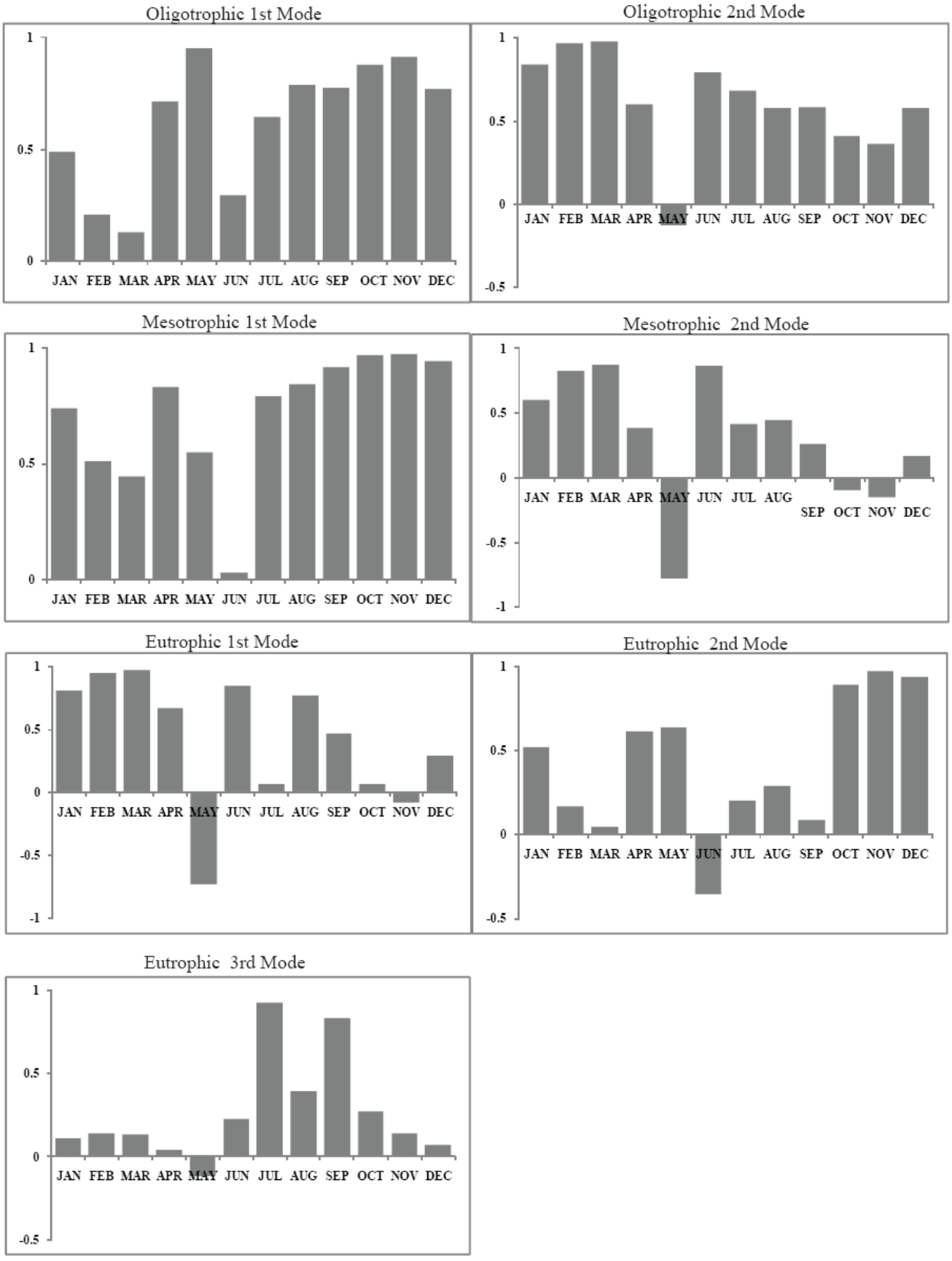
Oligotrophic 1st Mode
Oligotrophic 2nd Mode
Mesotrophic 1st Mode
Mesotrophic 2nd Mode
Eutrophic 1st Mode
Eutrophic 2nd Mode
Eutrophic 3rd Mode
JAN FEB MAR APR MAY JUN JUL AUG SEP OCT NOV DEC

Figure S7

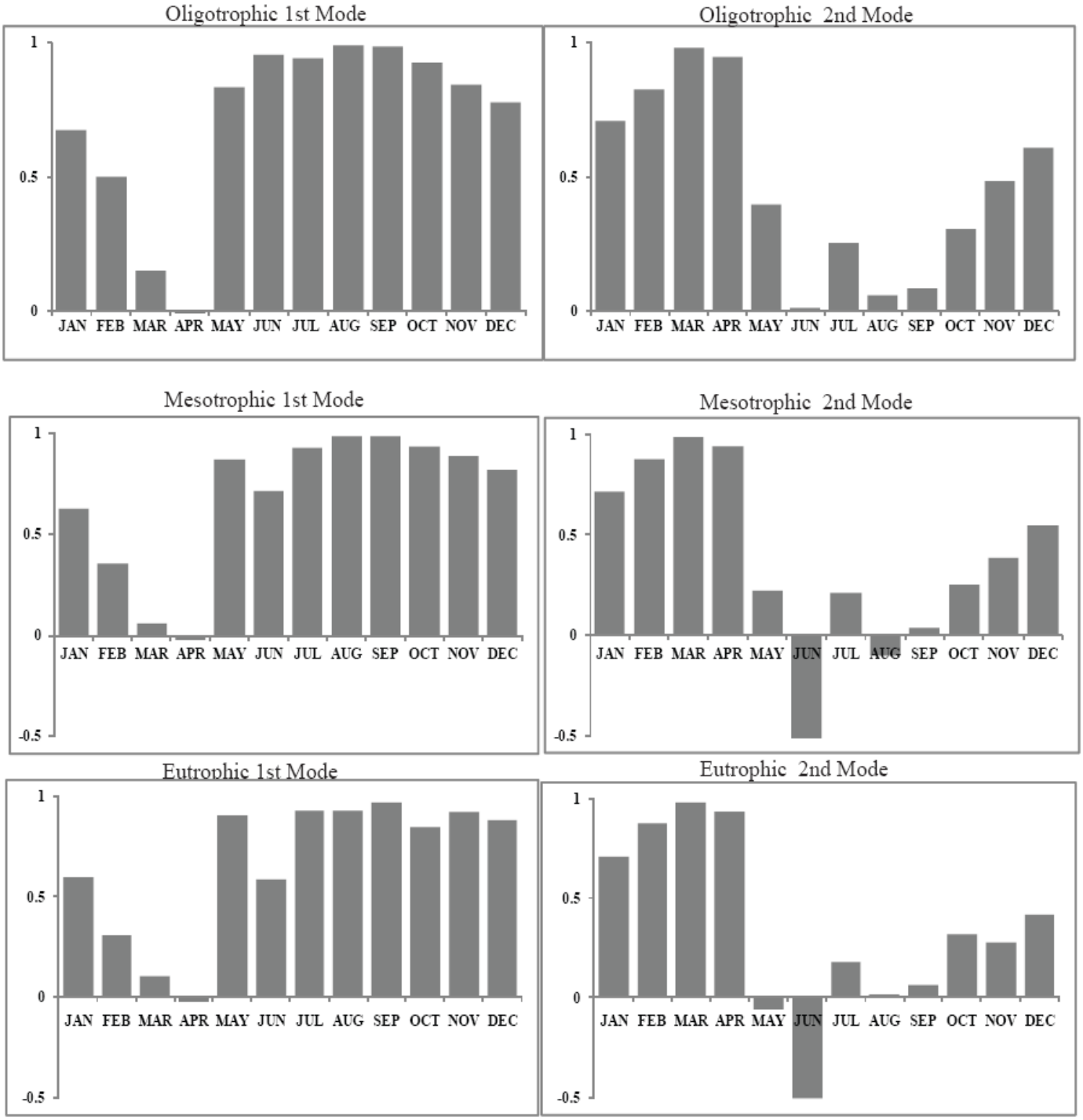
Oligotrophic 1st Mode
Oligotrophic 2nd Mode
Mesotrophic 1st Mode
Mesotrophic 2nd Mode
Eutrophic 1st Mode
Eutrophic 2nd Mode
1
0.5
0
-0.5
JAN FEB MAR APR MAY JUN JUL AUG SEP OCT NOV DEC

Figure S8

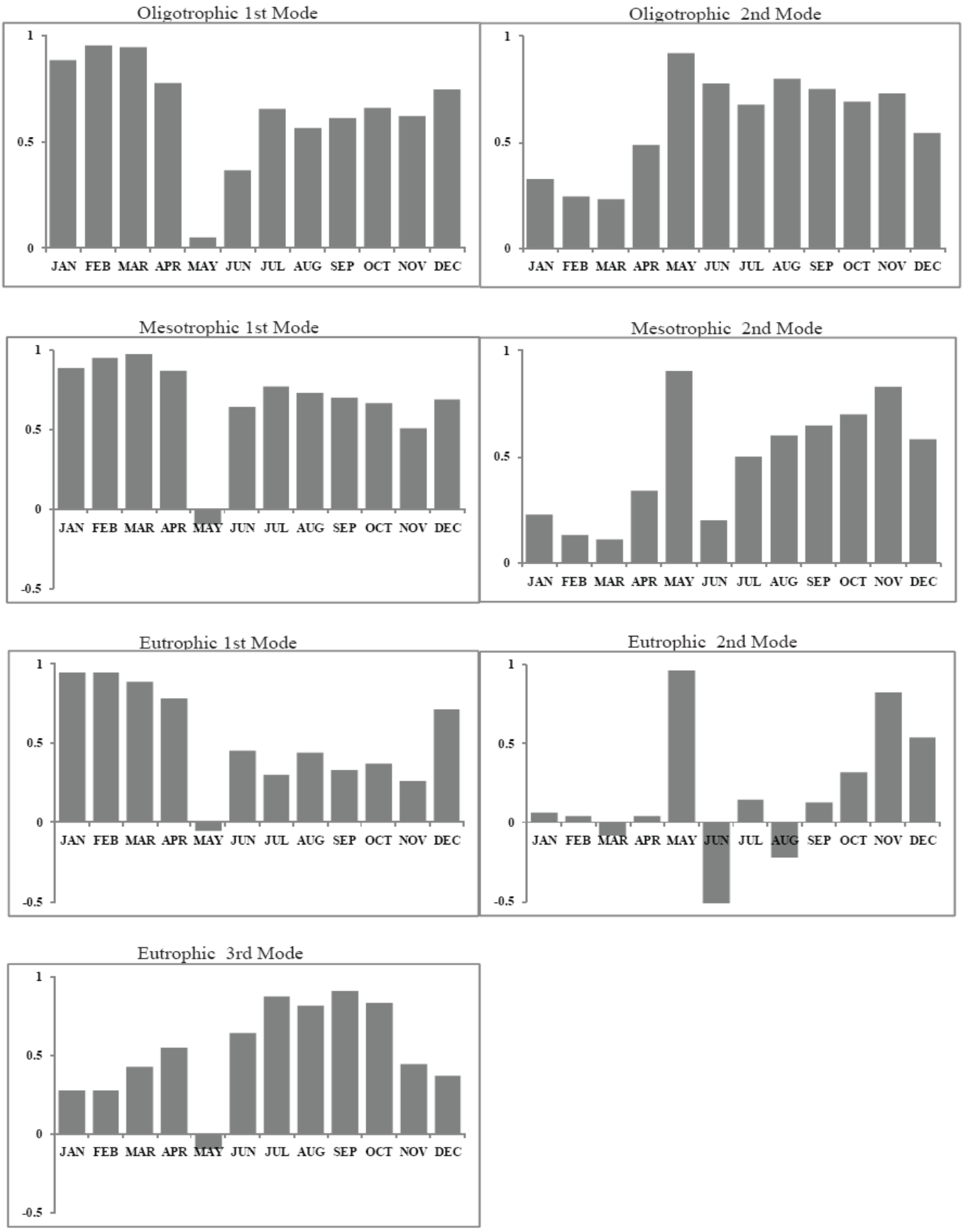
Oligotrophic 1st Mode
Oligotrophic 2nd Mode
Mesotrophic 1st Mode
Mesotrophic 2nd Mode
Eutrophic 1st Mode
Eutrophic 2nd Mode
Eutrophic 3rd Mode
1
0.5
0
-0.5
JAN FEB MAR APR MAY JUN JUL AUG SEP OCT NOV DEC

Figure S9

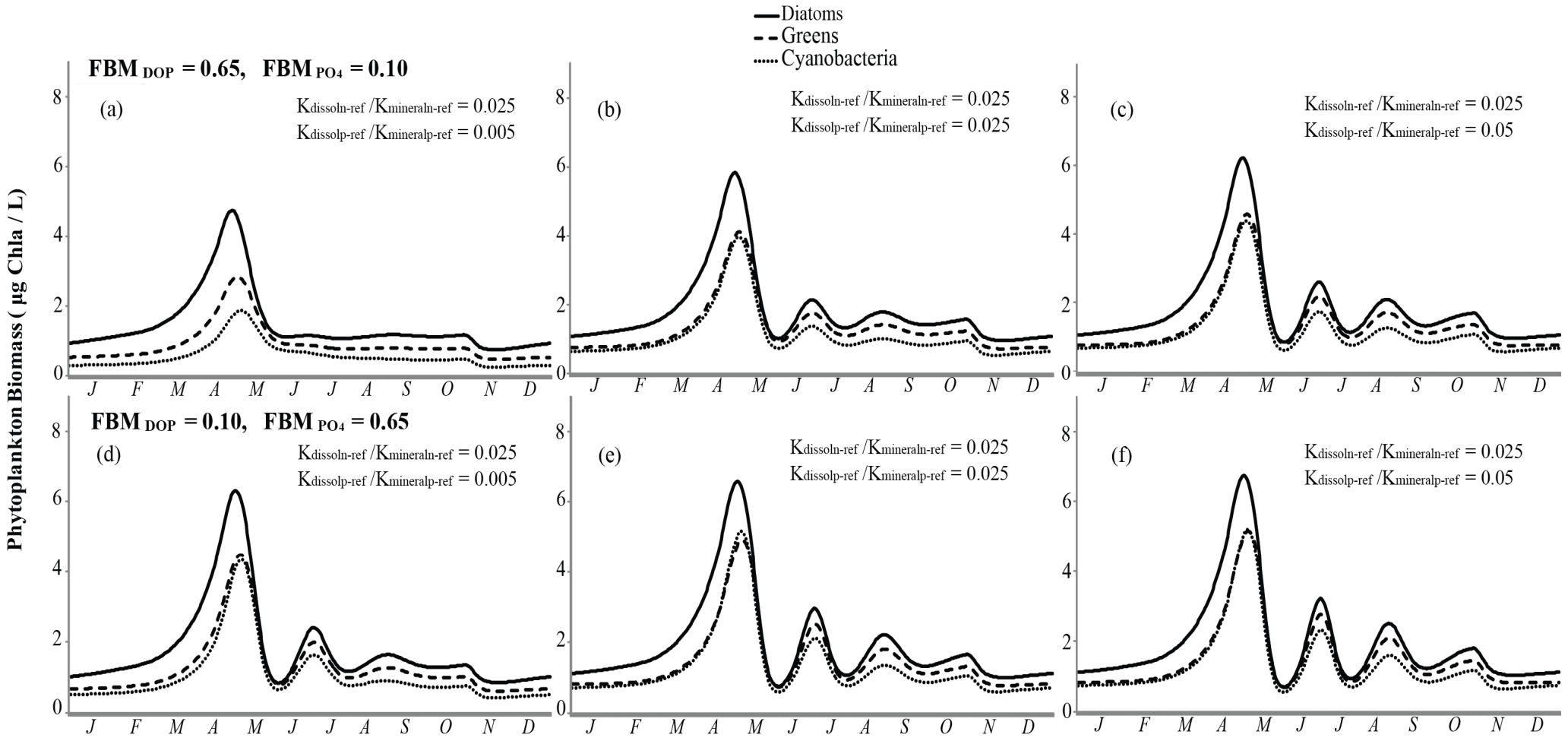
Diatoms
Greens
Cyanobacteria
Phytoplankton Biomass (µg Chla / L)
FBM DOP = 0.65, FBM PO4 = 0.10
(a)
Kdissoln-ref /Kmineraln-ref = 0.025
Kdissolp-ref /Kmineralp-ref = 0.005
(b)
Kdissoln-ref /Kmineraln-ref = 0.025
Kdissolp-ref /Kmineralp-ref = 0.025
(c)
Kdissoln-ref /Kmineraln-ref = 0.025
Kdissolp-ref /Kmineralp-ref = 0.05
FBM DOP = 0.10, FBM PO4 = 0.65
(d)
Kdissoln-ref /Kmineraln-ref = 0.025
Kdissolp-ref /Kmineralp-ref = 0.005
(e)
Kdissoln-ref /Kmineraln-ref = 0.025
Kdissolp-ref /Kmineralp-ref = 0.025
(f)
Kdissoln-ref /Kmineraln-ref = 0.025
Kdissolp-ref /Kmineralp-ref = 0.05
0
2
4
6
8
J F M A M J J A S O N D

Figure S10